論文 / 著書情報
Article / Book Information

題目(和文)	動的ネットワークシステムにおける制御器群の分散設計
Title(English)	Distributed Design of Controllers in Dynamical Network Systems
著者(和文)	笹原帆平
Author(English)	Hampei Sasahara
出典(和文)	学位:博士(工学), 学位授与機関:東京工業大学, 報告番号:甲第11128号, 授与年月日:2019年3月26日, 学位の種別:課程博士, 審査員:井村 順一,藤田 政之,三平 満司,山北 昌毅,早川 朋久,畑中 健志
Citation(English)	Degree:Doctor (Engineering), Conferring organization: Tokyo Institute of Technology, Report number:甲第11128号, Conferred date:2019/3/26, Degree Type:Course doctor, Examiner:,,,,,
学位種別(和文)	博士論文
Type(English)	Doctoral Thesis

Distributed Design of Controllers in Dynamical Network Systems

Hampei Sasahara

School of Engineering
Tokyo Institute of Technology

This dissertation is submitted for the degree of
Doctor of Engineering

February 2019

Abstract

This thesis provides a line of work on distributed design of structured controllers for large-scale dynamical network systems. Although most existing distributed controller design methods are built on the premise that the controllers are designed and integrated in a centralized manner, actual network systems are managed by multiple operators in many cases and each subcontroller is independently designed by its own operator based only on the model of the corresponding subsystem. In this thesis, novel distributed design methods for decentralized controllers and distributed controllers are proposed. An approach based on retrofit control is proposed for distributed design of decentralized controllers. The key idea is to regard the network system as an interconnected system among a subsystem of interest and the others and to attach a controller that preserves stability of the original network system. It is revealed that all retrofit controllers have a structure that rectifies the effect from the interconnection signal to the measurement signal. Moreover, to confirm the effectiveness of the proposed method, a numerical example through a benchmark model representing the bulk power system in the eastern half of Japan is shown. In addition, the results of retrofit control are generalized to glocal control where global and local controllers are designed in a distributed manner. Based on hierarchical representation, which is an equivalent representation of the original network system, a novel glocal control method is proposed.

Table of contents

Chapter 1

Introduction

1.1 Backgrounds

The thesis discusses control of large-scale dynamical network systems. A dynamical network system is composed of multiple dynamical subsystems and a network connecting the subsystems. Behavior of each subsystem's states obeys not only its own dynamics but also interaction among interconnected subsystems through the network. The notion of large-scale dynamical network systems covers a great variety of systems [1] and typical examples include power systems [2, 3], transportation systems [4], and social networks [5–7]. Safely operating such a large-scale network system with reliable control is an important issue because when a contingency happens at a part of the network system the failure widely spreads over the whole. In fact, serious blackouts caused by the cascading failure often happen throughout the world, such as the blackout of North America in 2003 where the number of affected people reaches into 45 million [8].

Although a great deal of effort has been devoted to the research of controller design in large-scale dynamical network systems, the problem still remains to be challenging. Several difficulties are arisen when controlling large-scale network systems and researchers in the filed of control engineering have mainly focused on the problem of information structure inside the designed controllers [9]. In the typical setting, it is supposed that a subcontroller is assigned to every subsystem and these controllers manage the whole network system in a coordinated manner by exchanging signal information with respect to its corresponding subsystem through communication with one another. Owing to the information exchange way, the structure of the controllers is restricted and hence the feasible set of designable controller is also limited. As a result, the mathematical problem of controller design is different from the classic one where no restriction on controller structure is placed. Several controller design methods, e.g., decentralized control and distributed control [10, 11], have been proposed to deal with information structure and the effectiveness has been verified.

Based on the existing results, the next issue to be resolved is *distributed design* of controllers [12], where each controller is designed in a distributed manner. In fact, most existing distributed controller design methods are built on the premise that the controllers are designed and integrated in a centralized manner; in other words, it is implicitly supposed that a single system operator manages the entire network system and designs all subcontrollers in the network system. Actual network systems, however, are managed by multiple operators in many cases and each subcontroller is independently designed by its own operator based only on the model of the corresponding subsystem. For instance, in power systems, multiple independent system operators exist and each of them is responsible for achieving supply-demand balance in its region while keeping the stability of the entire grid by subcontrollers, such as power system stabilizers (PSSs), which are designed independently [13]. Consequently, it is necessary to develop a distributed design method of controllers to deal with difficulties in real network systems.

The notion of distributed design has been proposed in [12] and the literature on this issue is still in its infancy. A distributed design method has been proposed in [12], but it places the unrealistic assumption that independent control inputs can be injected into every differential equation in the system. Although in [14] the authors have extended the result to the case of fully-actuated systems, the applicability is still limited. As another concept achieving distributed design, controller design methods based on system level synthesis [15–17] have been proposed. The key idea is to confine the closed-loop map to its local region and to make the optimal controller design problem separable and solvable locally. The approach can be applied only to discrete-time systems essentially and it cannot be determined in advance whether the optimization problem in the design process is feasible or not. In [18], a heuristic approach for designing intelligent balancing authorities that control subsystems inside each corresponding area to depress dynamic response to contingencies of interest is proposed. Although its effectiveness is shown numerically, no theoretical results are derived.

As a novel distributed design method of decentralized controllers, retrofit control [19, 20] has been recently proposed. The basic operation of retrofit control is to regard the system as an interconnected system among a subsystem of interest and the others and to design a retrofit controller that guarantees the entire system stability for any possible neighboring subsystems. Every operator in the targeted network system can independently design and implement a decentralized subcontroller while preserving the stability of the whole network system by employing retrofit controllers, which are designed based only on the model of the corresponding subsystem. Retrofit control requires no communication among sub-controllers, which has a potential of applicability to a large-class of interconnected systems, because all subcontrollers are purely decentralized and no lines are needed among the subcontrollers.

1.2 Contributions of Thesis

In view of the backgrounds mentioned in Section 1.1, the following problems are considered in this thesis.

First, we consider distributed design problem of decentralized controllers for a large-scale network system that is stably operated. There are multiple operators with the aim of suppressing effects of disturbance injected into the network system by implementing subcontrollers. Each operator can attach a subcontroller to the corresponding subsystem but the subcontroller design is performed based only on the subsystem model without the other subsystems and the network, called environment. The difficulty here is that existing controller design methods cannot deal with the unknown environment and even stability of the resulting system cannot be guaranteed with traditional ones. Under the situation, a controller design method for decentralized controllers in a distributed fashion that can assure the stability of the whole network system is proposed via retrofit control in this thesis.

Second, we consider the PSS design problem for frequency control in power grids with renewable energy resources. As a practical problem, stabilization of power grids to which large amount of distributed energy resources is introduced has been increasingly important. The frequencie of every synchronous generator in a large power grid is necessarily kept to be around the nominal value; otherwise these lose synchronism and a fatal fault, e.g., blackouts, occurs. Thus, it is extremely important to carefully design PSS that has the role to maintain the frequencies around the nominal value by measuring the corresponding generator's frequency and voltage and controlling the voltage injected into the automatic voltage regulator (AVR). Although existing design methods, e.g., a single-machine infinite-bus model [21], where the dynamics of the other parts is perfectly ignored for the controller design, work well for the traditional power grids, for future power grids where a large amount of renewable energy resources is installed controller design methods ought to be established via distributed design which gives assurance of the internal stability of the whole grids in a theoretical manner [22–24]. A numerical simulation is shown to demonstrate the effectiveness of our proposed approach for PSS design in power grids with renewable energy resources through IEEJ EAST 30-machine power system (EAST30) [25] with photovoltaic (PV) plants.

Finally, we consider the problem of integration of supervising controller design and decentralized local controller design for network systems. We refer to such a framework where a global controller spatially broadcasts the control inputs to the entire system and local decentralized controllers are simultaneously implemented as glocal control. The concept of glocal control has been already introduced in [26] but a systematic design of glocal controllers has not been established yet. Generalizing the results obtained for the above problems, we propose a novel glocal control that achieves distributed design of the controllers.

1.3 Organization

This thesis is organized as follows: First, in Chapter 2, a distributed design strategy of decentralized controllers via a newly defined retrofit control approach is proposed. To treat the network system mentioned in the previous section, we model the network system as an interconnected system with a valid model and an unknown environment that is assumed to be a system with which the entire system is stable. Under the setting, retrofit controllers are defined as the controllers that stabilize the interconnected system for any possible environment. A necessary and sufficient condition for retrofit controllers is derived based on Youla parameterization in an implicit form. Next, we define two kinds of retrofit controllers, output-rectifying retrofit controllers and input-rectifying retrofit controllers, to derive an explicit paramaterization of retrofit controllers. An explicit parameterization of all output-rectifying retrofit controllers is given under the assumption that the interconnection signal from the environment is available. It is found out that the structure inside all output-rectifying retrofit controllers is the proposed one in [19]. Owing to the parameterization, an optimal retrofit controller can be designed and consequently distributed design of decentralized controllers is achieved. Moreover, we show that similar structure is observed inside input-rectifying retrofit controllers as dual results.

In practical network systems, it is desirable to design a retrofit controller without the measurablity assumption on the interconnection signal because implementing sensors to obtain the interconnection signal often costs and it is sometimes impossible to measure the interconnection signal. In Chapter 3, we aim at relaxing the assumption and generalizing the result in Chapter 2. We consider the case where interconnection signal is unavailable and derive a parameterization of all state-feedback retrofit controllers without interconnection signal. It is shown that a similar structure can be observed in all state-feedback retrofit controllers to that of retrofit controllers with interconnection signals.

In Chapter 4, for the purpose of treating the stabilization problem for power grids, we first give a mathematical model of EAST30 composed of synchronous machines, loads, PV generators in addition to buses that form the network. The dynamics with respect to synchronous machines is a 13-dimensional dynamical system each of which is composed of a synchronous generator, an excitation system with AVR, and a turbine with governor. The loads and PV power plants are modeled as constant loads and constant power sources, respectively. We show that the power grid can be regarded as an interconnected system treated in Chapter 2 and 3 and apply the proposed approach for PSS design. A numerical simulation is shown to demonstrate the effectiveness of our proposed approach for PSS design in power grids with renewable energy resources through the PV-integrated EAST30 model [25].

We generalize the above approach to glocal (global/local) control, where spatially distributed decentralized controllers and a central broadcasting controller cooperatively manage the entire network system, in Chapter 5. A novel glocal control method based on hierarchical representation, whose notion is introduced in this work, is proposed. Given the definition of hierarchical representation, we derive a necessary and sufficient condition for existence of hierarchical representation for a network system. Based on the hierarchical representation, we propose a linear function observer that preserves the hierarchical structure and distributed design of global and local controllers is achieved with the observer. The design procedure of controllers are independently performed and it indicates that the controllers can be designed in a distributed manner. It is shown that both of local and global behaviors are simultaneously suppressed thanks to the existence of the global controller. A numerical example with EAST30 is shown to illustrate the effectiveness of the proposed glocal control method.

Finally, Chapter 6 draws conclusion.

NOTATION: The following notation is to be used through the thesis:

$\mathbb{R}$	the set of real numbers
$\mathbb{C}$	the set of complex numbers
$\mathcal{L}_2$	the set of all square integrable functions
$\mathcal{R}^{n\times m}$	the set of real and rational $n \times m$ transfer matrices
$\mathcal{RP}^{n\times m}$	the set of proper transfer matrices in $\mathcal{R}^{n\times m}$
$\mathcal{RH}_\infty^{n\times m}$	the set of stable transfer matrices in $\mathcal{RP}^{n\times m}$
$\lvert\mathcal{I}\rvert$	the cardinality of a set $\mathcal{I}$
$\dim(\mathcal{X})$	the dimension of a vector space $\mathcal{X}$
$\mathcal{X}^\perp$	the orthogonal subspace of a subspace $\mathcal{X}$
$\mathcal{X}+\mathcal{Y}$	the sum space of subspaces $\mathcal{X}$ and $\mathcal{Y}$
$\boldsymbol{j}$	the imaginary unit
$\boldsymbol{x}^*$	the conjugate of $\boldsymbol{x} \in \mathbb{C}$
$\lvert\boldsymbol{x}\rvert$	the absolute value of $\boldsymbol{x} \in \mathbb{C}$
$\angle\boldsymbol{x}$	the angle of $\boldsymbol{x} \in \mathbb{C}$
$\mathrm{Re}\,\boldsymbol{x}$ $(\mathrm{Im}\,\boldsymbol{x})$	the real (imaginary) value of $\boldsymbol{x} \in \mathbb{C}$
$\mathbf{comp}(x)$	$[1\ \boldsymbol{j}]x$ for $x \in \mathbb{R}^2$
$\lVert x\rVert$	the Euclidean norm of a vector x
$\mathrm{col}(x_i)_{i\in\mathcal{I}}$	the vector where x_i for $i \in \mathcal{I}$ are arranged in vertical
I_n	the n-dimensional identity matrix
M^T	the transpose of a matrix M
$M^\dagger$	a pseudo inverse of a full rank matrix M
$\mathrm{im}\,M$	the image of a matrix M
$\ker M$	the kernel of a matrix M
$\lVert M\rVert$	the maximum singular value of a matrix M
$M \otimes N$	the Kronecker product of matrices M and N
$\sigma(M)$	the spectrum of a matrix M
$\det(M)$	the determinant of a matrix M
$\mathrm{diag}(M_1,\dots,M_n)$	the block diagonal matrix whose diagonal blocks are composed of matrices $M_1,\dots,M_n$
$\mathcal{R}(A,B)$	the controllable subspace with respect to the pair (A,B)

When the dimensions are clear from the context, we omit the superscript and the subscript, e.g., employing $\mathcal{RH}_\infty$ instead of $\mathcal{RH}_\infty^{n\times m}$. The $\mathcal{L}_2$-norm of a square-integrable function $f \in \mathcal{L}_2$ is defined by

$$\lVert f\rVert_2 := \sqrt{\int_0^\infty \lVert f(t)\rVert^2 dt}$$

and the $\mathcal{H}_2$-norm and $\mathcal{H}_\infty$-norm of a transfer matrix G are defined by

$$\|G\|_2 := \sqrt{\frac{1}{2\pi}\int_{-\infty}^{\infty} \operatorname{tr}\left(G(\boldsymbol{j}\omega)G(\boldsymbol{j}\omega)^{\mathsf{T}}\right) d\omega}, \quad \|G\|_\infty := \sup_{\omega\in\mathbb{R}} \|G(\boldsymbol{j}\omega)\|,$$

respectively. The lower and the upper linear fractional transformations (LFTs) [27] are defined by

$$\mathcal{F}_{\mathrm{l}}(M,N) := M_{11} + M_{12}N(I - M_{22}N)^{-1}M_{21},$$
$$\mathcal{F}_{\mathrm{u}}(M,N) := M_{22} + M_{21}N(I - M_{11}N)^{-1}M_{12},$$

respectively, where $M_{11}, M_{12}, M_{21}, M_{22}$ are defined by

$$M = \begin{bmatrix} M_{11} & M_{12} \\ M_{21} & M_{22} \end{bmatrix}$$

whose dimensions are compatible with N, provided that the inverses exist. When a transfer function G has a realization $C(sI - A)^{-1}B + D$, the shorthand is defined by

$$\left[\begin{array}{c|c} A & B \\ \hline C & D \end{array}\right] := G.$$

In this thesis, all physical quantities such as the voltage V, are represented in per unit and the unit is omitted when it is clear from the context. The superscript $\star$ represents setpoints; for example, $P^\star$ denotes the setpoint of P.

Chapter 2

Distributed Design of Local Controllers via Retrofit Control

2.1 Introduction

In this chapter, a distributed design strategy of local controllers via retrofit control is proposed. We consider a stably operated network system where there are multiple operators whose aim is to suppress effects of disturbance injected into the network system by implementing subcontrollers while preserving the stability. We stand in an individual operator's point and treat the network system as an interconnected system that consists of the subsystems of interest and an unknown environment. The prior information that the entire system is stable leads to the assumption that the environment belongs to the set of systems with which the entire network system is internally stable. We give a new definition of retrofit controllers as controllers that preserve the stability of the entire network system for any possible environment and then derive a necessary and sufficient condition for retrofit controllers based on Youla parameterization. Next, we introduce two kinds of retrofit controllers, output-rectifying retrofit controllers and input-rectifying retrofit controllers. We show that a certain clear structure can be observed inside all output-rectifying retrofit controllers and dual results can be obtained for input-rectifying retrofit controllers.

This chapter is organized as follows. In Section 2.2, we give the system model treated in this chapter and the definition of retrofit controllers. Section 2.3 derives a characterization of all retrofit controllers in the frequency domain based on Youla parameterization. In Section 2.4, we introduce the notion of output-rectifying retrofit controllers and input-rectifying retrofit controllers and identify the structure that must be inside all output-rectifying retrofit controllers with interconnection signal. Moreover, in Section 2.5, we overview dual results found in input-rectifying retrofit controllers. Finally, Section 2.6 concludes this chapter.

2.2 Retrofit Control

2.2.1 System Model

We consider linear time-invariant interconnected systems illustrated by Fig. 2.1, where the system is given by

$$G_{\rm pre}:\begin{cases}\begin{bmatrix} w \\ z \\ y \end{bmatrix} = G\begin{bmatrix} v \\ d \\ u \end{bmatrix}, \\ \quad v \quad = G_{\rm E} w, \end{cases} \tag{2.1}$$

v, w, are interconnection signals, z is the evalulated output, d is the external disturbance, y is the measurement output, u is the control input, $G, G_{\rm E}$ are transfer matrices of the subsystems, G is given by

$$G = \begin{bmatrix} G_{wv} & G_{wd} & G_{wu} \\ G_{zv} & G_{zd} & G_{zu} \\ G_{yv} & G_{yd} & G_{yu} \end{bmatrix}.$$

For ease of discussion, we assume that well-posedness is guaranteed for any feedback system in this thesis. We refer to $G, G_{\rm E}$ and $G_{\rm pre}$ as a local system, an environment, and a preexisting system, respectively. The local system is connected to the environment through interconnection signals and these systems form the preexisting system. In the setting, the local system represents a subsystem managed by a single operator whereas the environment includes the other subsystems and also the other sub-controllers implemented by the other operators. Suppose that the interconnected system stably operates and our aim is to design a dynamic controller K that generates the feedback control

$$u = Ky \tag{2.2}$$

to improve control performance, namely, $\mathcal{L}_2$-norm of the transfer function from d to z, while preserving the entire system stability. The signal-flow diagram of the entire system is shown in Fig. 2.2.

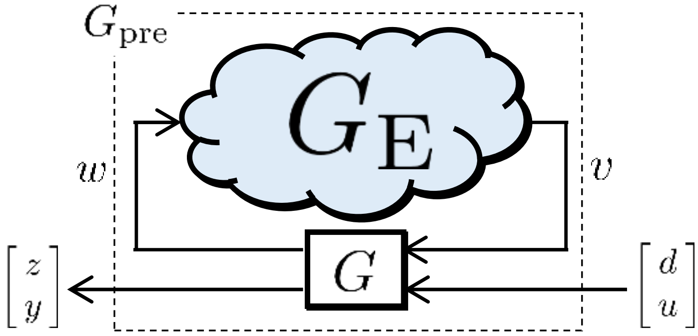

Fig. 2.1 The signal-flow diagram of the interconnected system between the local system G and an environment $G_{\rm E}$.

2.2.2 Definition of Retrofit Controllers

When we can use the model of the system of (2.1) for design of the controller, many controller design methods such as $\mathcal{H}_\infty$ optimal control can be utilized. It is, however, difficult to grasp the model information of the whole system when the system represents a large-scale network system where there are multiple managers such as power systems. The environment possibly varies due to others' control action even if the designer can obtain the model information of the whole system at some time instant. This fact indicates that it is impossible to follow all variations of the network system under control by multiple operators. Following the circumstance, we suppose that the entire model of the network system is unavailable. Instead, we assume that only the model information of G is available and the environment $G_{\rm E}$ can be any transfer matrix in compliance with keeping the preexisting system to be stable. In other words, we suppose that $G_{\rm E}$ can be taken as any element of the set $\mathcal{G}_{\rm E}$ where

$$\mathcal{G}_{\rm E} := \{G_{\rm E} \in \mathcal{RP} : G_{\rm pre} \text{ is internally stable}\}.$$

We refer to a notion of control under the restriction on system model information as *retrofit control* and controllers that guarantee the entire system stability for any possible environment as *retrofit controllers*. The precise definition of retrofit controllers is given as follows.

Definition 1 *A controller K in* (2.2) *is called a retrofit controller with respect to G, when the system in Fig. 2.2 is internally stable for any $G_{\rm E} \in \mathcal{G}_{\rm E}$.*

One may think that the definition of retrofit controllers can be treated as a kind of robust stabilizing controllers in the sense that retrofit controllers guarantee the

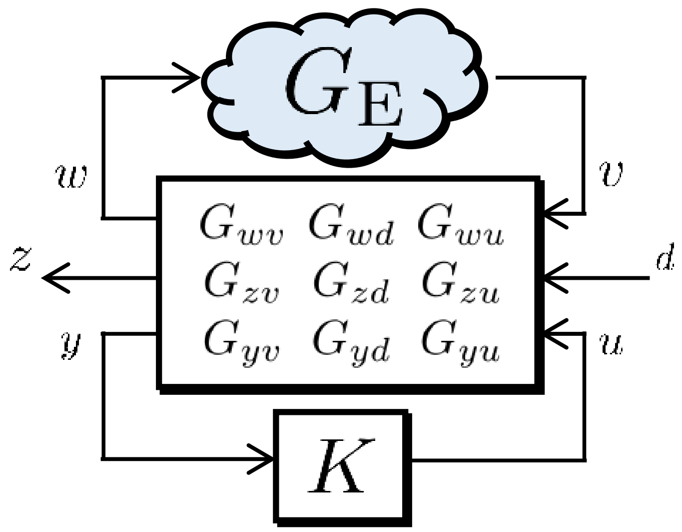

Fig. 2.2 The signal-flow diagram of the closed-loop system.

internal stability of the whole system for any possible unknown perturbation. Retrofit controllers are, however, essentially different from conventional robust controllers since the set of perturbations is characterized by the systems that make the preexisting open-loop system internally stable. On the other hand, in the setting of typical robust control, e.g., $\mathcal{H}_\infty$ control, the perturbation is represented by the set of plants whose norm is bounded.

In the following part, we develop a retrofit control for distributed design. We derive a mathematical characterization of the retrofit controllers and a parameterization of all retrofit controllers with a constrained design parameter. We also show that the local closed-loop map from d to z can be represented with affine functions in terms of the design parameter of retrofit controllers.

2.3 Characterization of All Retrofit Controllers

In the previous section, the definition of retrofit controllers is given. In this section, we derive a necessary and sufficient condition for retrofit controllers. Before proceeding to the main theorem, we note that the set of environments can be characterized based on the Youla parameterization [28]. For the sake of simplicity, the following assumption is made throughout this chapter:

Assumption 1 *The local system is stable; that is, G belongs to $\mathcal{RH}_\infty$.*

Under Assumption 1, the Youla parameterization with respect to G_{E} has a simple form as follows. For any $G_{\mathrm{E}} \in \mathcal{G}_{\mathrm{E}}$, there exists $Q_{\mathrm{E}} \in \mathcal{RH}_\infty$ such that $G_{\mathrm{E}} = (I +$

$Q_{\rm E}G_{wv})^{-1}Q_{\rm E}$ and conversely for any $Q_{\rm E} \in \mathcal{RH}_\infty$ there exists $G_{\rm E} \in \mathcal{G}_{\rm E}$ satisfying $Q_{\rm E} = (I - G_{\rm E}G_{wv})^{-1}G_{\rm E}$. Thus the set $\mathcal{G}_{\rm E}$ can be characterized by

$$\mathcal{G}_{\rm E} = \{(I + Q_{\rm E}G_{wv})^{-1}Q_{\rm E} \in \mathcal{RP} : Q_{\rm E} \in \mathcal{RH}_\infty\}.$$

We hereafter refer to $Q_{\rm E}$ as the Youla parameter with respect to G_{wv}. Note that this assumption is not very essential and the extended results are shown in Chapter 4.

2.3.1 Characterization of All Retrofit Controllers

A characterization of all retrofit controllers is given by the following theorem.

Theorem 1 *Consider the interconnected system in Fig. 2.2. Under Assumption 1, the controller K is a retrofit controller if and only if there exists $Q \in \mathcal{RH}_\infty$ such that*

$$K = Q(I + G_{yu}Q)^{-1} \tag{2.3}$$

and

$$G_{wu}QG_{yv} = 0. \tag{2.4}$$

Proof: (sufficiency) We first prove the sufficiency that if there exists $Q \in \mathcal{RH}_\infty$ such that the condition (2.4) holds then K is a retrofit controller. Note that Q is the Youla parameter with respect to G_{yu} given by

$$Q = (I - KG_{yu})^{-1}K.$$

Because for any $G_{\rm E}$ in $\mathcal{G}_{\rm E}$, $K = 0$ achieves the internal stability of the entire system, the system in Fig. 2.2 is stabilizable with respect to K for any $G_{\rm E}$ in $\mathcal{G}_{\rm E}$. Hence the internal stability of the system in Fig. 2.2 is equivalent to that of the system in Fig. 2.3 from Lemma 12.2 in [27]. The internal stability of the system is equivalent to that the sixteen transfer matrices from $\delta_u, \delta_y, \delta_v, \delta_w$ to u, y, v, w belong to $\mathcal{RH}_\infty$.

First, we focus on the signal w. From the block diagram in Fig. 2.3,

$$w = (G_{wu}QG_{yv}G_{\rm E} + G_{wv}G_{\rm E})w + G_{wu}(I - KG_{yu})^{-1}\delta_u + G_{wu}Q\delta_y + G_{wv}\delta_v + \delta_w.$$

The condition (2.4) implies that

$$\begin{aligned} w =\ & (I - G_{wv}G_{\rm E})^{-1}G_{wu}(I - KG_{yu})^{-1}\delta_u + (I - G_{wv}G_{\rm E})^{-1}G_{wu}Q\delta_y \\ & + (I - G_{wv}G_{\rm E})^{-1}G_{wv}\delta_v + (I - G_{wv}G_{\rm E})^{-1}\delta_w. \end{aligned} \tag{2.5}$$

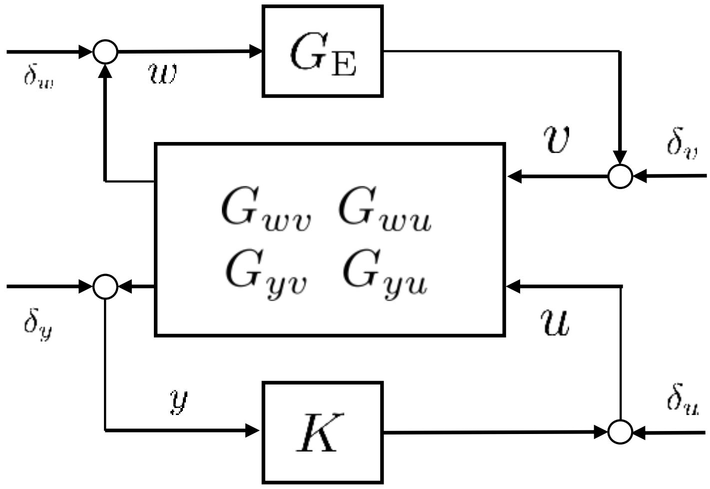

Fig. 2.3 An equivalent system to that in Fig. 2.2 for stability analysis.

Using the relations

$$(I - G_{wv}G_{\rm E})^{-1} = I + G_{wv}Q_{\rm E}, \quad (I - KG_{yu})^{-1} = I + QG_{yu},$$

the relationship (2.5) can be transformed into

$$w = (I+G_{wv}Q_{\rm E})G_{wu}(I+QG_{yu})\delta_u+(I+G_{wv}Q_{\rm E})G_{qu}Q\delta_y+Q_{\rm E}\delta_v+(I+G_{wv}Q_{\rm E})\delta_w. \quad (2.6)$$

Because Q and $Q_{\rm E}$ belong to $\mathcal{RH}_\infty$, the stability of G implies that the transfer matrices in (2.6) belong to $\mathcal{RH}_\infty$. With (2.6), we have

$$v = Q_{\rm E}G_{wu}(I + QG_{yu})\delta_u + Q_{\rm E}G_{wu}Q\delta_y + (I + Q_{\rm E}G_{wv})\delta_v + Q_{\rm E}\delta_w.$$

This fact results in that the transfer matrices from $\delta_u, \delta_y, \delta_v, \delta_w$ to v, w belong to $\mathcal{RH}_\infty$. Hence, the relationship

$$\begin{cases} u = (I + QG_{yu})\delta_u + Q\delta_y + QG_{yv}v, \\ y = (I + G_{yu}Q)G_{yu}\delta_u + (I + G_{yu}Q)\delta_y + (I + G_{yu}Q)G_{yv}v \end{cases}$$

implies that all of the transfer matrices from $\delta_u, \delta_y, \delta_v, \delta_w$ to u, y, v, w belong to $\mathcal{RH}_\infty$. Therefore, the system in Fig. 2.3 is internally stable for any $G_{\rm E}$ in $\mathcal{G}_{\rm E}$, that is, K is a retrofit controller if Q belongs to $\mathcal{RH}_\infty$ and the condition (2.4) is satisfied.

(necessity) We next show the necessity that if K is a retrofit controller then Q belongs to $\mathcal{RH}_\infty$ and the condition (2.4) is satisfied.

First, we take $G_{\mathrm{E}} = 0 \in \mathcal{G}_{\mathrm{E}}$. Since K is a retrofit controller, the system in Fig. 2.3 is internally stable in this case. Then the relationship from δ_u and δ_u to u and y can be written by

$$\begin{cases} u = (I - KG_{yu})^{-1}\delta_u + Q\delta_y, \\ y = (I - G_{yu}K)^{-1}G_{yu}\delta_u + (I - G_{yu}K)^{-1}\delta_y. \end{cases}$$

Due to the internal stability, the matrix from δ_y to u necessarily belongs to $\mathcal{RH}_\infty$ and this leads to that Q belongs to $\mathcal{RH}_\infty$.

We next show that the condition (2.4) is satisfied. Define $T_{\mathrm{loop}} := G_{wu}QG_{yv}$. Then the relation from δ_w to v is given by $(I - Q_{\mathrm{E}}T_{\mathrm{loop}})^{-1}Q_{\mathrm{E}}$. The internal stability implies that

$$(I - Q_{\mathrm{E}}T_{\mathrm{loop}})^{-1}Q_{\mathrm{E}} \in \mathcal{RH}_\infty. \tag{2.7}$$

Now consider $(I - Q_{\mathrm{E}}T_{\mathrm{loop}})^{-1}$ and then

$$(I - Q_{\mathrm{E}}T_{\mathrm{loop}})^{-1} = I + (I - Q_{\mathrm{E}}T_{\mathrm{loop}})^{-1}Q_{\mathrm{E}}T_{\mathrm{loop}} \in \mathcal{RH}_\infty$$

holds because (2.7) holds and T_{loop} belongs to $\mathcal{RH}_\infty$.

Finally, supposing

$$T_{\mathrm{loop}} \neq 0 \tag{2.8}$$

we construct an environment $G_{\mathrm{E}} \in \mathcal{G}_{\mathrm{E}}$ that destabilizes $(I - Q_{\mathrm{E}}T_{\mathrm{loop}})^{-1}$. Under the condition (2.8), there exists Q_{E} in $\mathcal{RH}_\infty$ such that

$$\det(I - Q_{\mathrm{E}}(\boldsymbol{j}\omega)T_{\mathrm{loop}}(\boldsymbol{j}\omega)) = 0$$

for some $\omega \in \mathbb{R}$ as in the proof of the small-gain theorem (for example, see Theorem 9.1 in [27]). For such Q_{E}, the transfer matrix $(I - Q_{\mathrm{E}}T_{\mathrm{loop}})^{-1}$ does not belong to $\mathcal{RH}_\infty$. This is a contradiction and T_{loop} must be zero. Therefore, the condition (2.4) holds if the system in Fig. 2.3 is internally stable for any $G_{\mathrm{E}} \in \mathcal{G}_{\mathrm{E}}$. □

Theorem 1 gives a constrained version of the Youla parameterization of all stabilizing controllers that can cope with the unknown environment. An intuitive interpretation of the claim of Theorem 1 can be explained as follows. Omitting d and z, we have the closed-loop system depicted by the left part of Fig. 2.4. Based on the Youla parameterization, we can obtain an equivalent system shown in the right part of Fig. 2.4. The condition (2.4) indicates that the loop transfer matrix becomes a zero matrix and hence the closed-loop system is internally stable for any environment. On the other hand, if the condition (2.4) is not satisfied, then there exists Q_{E} such that

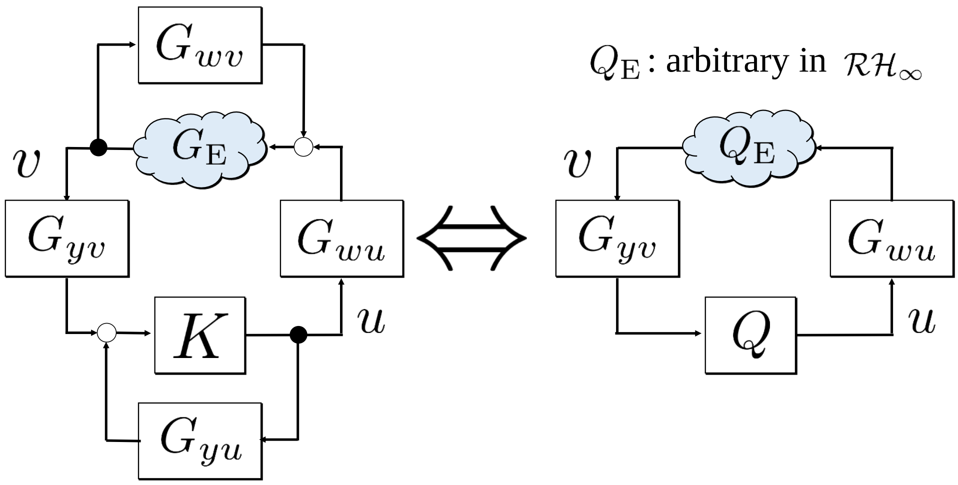

Fig. 2.4 Equivalent closed-loop systems

the system becomes unstable because Q_E can be chosen as any element of $\mathcal{RH}_\infty$ from the definition of $\mathcal{G}_E$. Thus, the condition (2.4) is also a necessary condition for retrofit controllers.

2.3.2 Closed-Loop Map with Retrofit Controller and Difficulty on Retrofit Controller Design

The closed-loop map of the entire system with a retrofit controller is given by the following theorem.

Theorem 2 *Let $T_{\rm all}$ be the closed-loop map from the external disturbance d to the evaluated output z. If K is a retrofit controller, then*

$$T_{\rm all} = T_{zd}(Q) + T_{zv}(Q) Q_E T_{wd}(Q) \tag{2.9}$$

where

$$\begin{aligned} T_{zd}(Q) &:= G_{zd} + G_{zu} Q G_{yd}, \\ T_{zv}(Q) &:= G_{zv} + G_{zu} Q G_{yv}, \\ T_{wd}(Q) &:= G_{wd} + G_{wu} Q G_{yd}. \end{aligned}$$

Proof: By definition, we have

$$\begin{aligned}
T_{\rm all} &= \mathcal{F}_{\rm l}(G_{\rm pre}, K) \\
&= \mathcal{F}_{\rm l}(\mathcal{F}_{\rm u}(G, G_{\rm E}), K) \\
&= \mathcal{F}_{\rm u}(\mathcal{F}_{\rm l}(G, K), G_{\rm E}) \\
&= \mathcal{F}_{\rm u}\left(\begin{bmatrix} G_{wv} & G_{wd} \\ G_{zv} & G_{zd} \end{bmatrix} + \begin{bmatrix} G_{wu} \\ G_{zu} \end{bmatrix} Q[G_{wv}\ G_{yd}], G_{\rm E}\right) \\
&= G_{zd} + G_{zu}QG_{yd} \\
&\quad +(G_{zv} + G_{zu}QG_{yv})G_{\rm E}\{I - (G_{wv} + G_{wu}QG_{yv})G_{\rm E}\}^{-1})(G_{wd} + G_{wu}QG_{yd}).
\end{aligned}$$

From the assumption that K is a retrofit controller and Theorem 1, $G_{wu}QG_{yv} = 0$ and hence $T_{\rm all}$ can be written as (2.9). □

The closed-loop map with a retrofit controller is an affine function of $Q_{\rm E}$ and transfer matrices T_{zd}, T_{zv}, T_{wd} are also affine functions of Q while this property is not satisfied when a general controller is employed. From Theorem 2, it is expected that the entire closed-loop performance is improved by simply choosing Q so as to suppress the affine transfer matrices. Note that those transfer matrices represent the local closed-loop maps composed of G and K from the external input and the interconnection signal from the environment to the evaluated output and the interconnection signal from the local system. Consequently, it is indicated that we have to take not only d and z but also v and w into account for control performance. Conversely, it is also shown that the only alternative to deal with the varying environment is to simultaneously suppress the transfer matrices.

It has been revealed that the retrofit controller design problem is reduced to the problem to find $Q \in \mathcal{RH}_\infty$ such that norms of the transfer matrices in (2.9) are small under the constraint (2.4). The design problem, however, cannot be handled by a standard controller design method even though the optimization problem is convex owing to the existence of the condition (2.4). One approach to overcome the difficulty is to provide an explicit representation of all solutions to the equation (2.4) but this approach is severe in general. In fact, all solutions to the equation (2.4) in $\mathcal{R}$ can be represented by the form

$$Q = Q_0 - G_{wu}^{\dagger} G_{wu} Q_0 G_{yv} G_{yv}^{\dagger} \in \mathcal{R} \tag{2.10}$$

where $G_{wu}^{\dagger}$ and $G_{yv}^{\dagger}$ are the generalized inverses of G_{wu} and G_{yv}, respectively, and Q_0 is an arbitrary transfer matrix provided that G_{wu} and G_{yv} are full-row and full-column rank (See Fact 6.4.43 in [29]). However, it is difficult to design a retrofit controller by directly utilizing (2.10) for the following two reasons. First, solutions derived by (2.10) are not guaranteed to be proper and stable because the generalized inverses are possibly improper or unstable. Second, the design parameter in (2.10) is represented by Q_0 and the transfer matrices in (2.9) are no longer affine functions with respect to the design parameter.

The above discussion indicates that retrofit controller design is a hard problem to solve in the general case. To resolve this issue, in the next section we consider two classes of retrofit controllers and derive explicit representations for the classes of retrofit controllers with which the design problem is reduced to be a standard problem.

2.4 Design of Output-Rectifying Retrofit Controllers with Interconnection Signal

In this section, we consider two classes of retrofit controllers and show that the retrofit controllers of the classes can be parameterized with a local stabilizing controller. It has been already shown that a retrofit controller can be designed by letting the controller have a structure shown below in [19]. We reveal that the structure is not only sufficient but also necessary for a class of retrofit controllers.

2.4.1 Definition of Output-Rectifying Retrofit Controllers and Input-Rectifying Retrofit Controllers

Now we define two kinds of retrofit controllers, namely, *output-rectifying retrofit controllers* and *input-rectifying retrofit controllers*.

Definition 2 *A controller K is said to be an output-rectifying retrofit controller, if there exists $Q \in \mathcal{RH}_\infty$ such that* (2.3) *holds and*

$$QG_{yv} = 0. \tag{2.11}$$

Similarly, a controller K is said to be an input-rectifying retrofit controller, if there exists $Q \in \mathcal{RH}_\infty$ such that (2.3) *holds and*

$$G_{wu}Q = 0. \tag{2.12}$$

Obviously, those controllers are retrofit controllers because the conditions (2.11) and (2.12) are sufficient conditions for the condition (2.4). The reason why the controllers satisfying (2.11) are referred to as output-rectifying retrofit controllers is that the measurement output is rectified inside the controller such that the effect from the interconnection signal from the environment v is eliminated. Similarly, the controllers satisfying (2.12) are referred to as input-rectifying retrofit controllers because the control input is rectified such that the input does not affect the interconnection signal to the environment w at all.

2.4.2 Parameterization of All Output-Rectifying Retrofit Controllers with Interconnection Signal

We attempt to provide an unconstrained parameterization of all output-rectifying retrofit controllers. We first consider the special case where the interconnection signal v is available at the controller; that is, the control input can be represented by

$$u = K \begin{bmatrix} y \\ v \end{bmatrix}. \tag{2.13}$$

It is shown that all output-rectifying retrofit controllers can be parameterized with a local stabilizing controller under the measurability of the interconnection signal. We also show that all output-rectifying retrofit controllers with interconnection measurement have a specific structure composed of a local staibilizing controller and an output rectifier, defined below. This case under the assumption that the interconnection signal can be fed back has not only advantage to simplify the results but also implication for more general cases.

The following theorem gives an unconstrained parameterization of all output-rectifying retrofit controllers with interconnection measurement.

Theorem 3 *Under the assumption that the interconnection signal v can be fed back and K can be represented as* (2.13)*, the controller K is an output-rectifying retrofit controller if and only if the controller has the form*

$$K = \hat{K} G_{\mathrm{R}} \tag{2.14}$$

where $\hat{K}$ is a controller that stabilizes G_{yu} with

$$G_{\mathrm{R}} := [I \;\; -G_{yv}].$$

Proof: First of all, we define the transfer matrices $G_{(y,v)v}$, $G_{(y,v)d}$, and $G_{(y.v)u}$ by

$$\begin{bmatrix} y \\ v \end{bmatrix} = \begin{bmatrix} G_{(y,v)v} \ G_{(y,v)d} \ G_{(y.v)u} \end{bmatrix} \begin{bmatrix} v \\ d \\ u \end{bmatrix}.$$

Specifically, those transfer matrices are given by

$$G_{(y,v)v} = \begin{bmatrix} G_{yv} \\ I \end{bmatrix}, \ G_{(y,v)d} = \begin{bmatrix} G_{yd} \\ 0 \end{bmatrix}, \ G_{(y,v)u} = \begin{bmatrix} G_{yv} \\ 0 \end{bmatrix}.$$

Note that the condition for output-rectifying retrofit controllers (2.11) is rewritten by

$$QG_{(y,v)v} = 0 \tag{2.15}$$

with $Q := (I - KG_{(y,v)u})^{-1}K$ under the assumption that v can be fed back.

Assume that $Q \in \mathcal{RH}_\infty$ and the condition (2.15) is satisfied. Suppose K can be divided by

$$K = \begin{bmatrix} \hat{K} \ \hat{K}_v \end{bmatrix}$$

with transfer matrices $\hat{K}$ and $\hat{K}_v$ whose dimensions are compatible with y and v, respectively. Note that the condition (2.15) is equivalent to

$$\begin{bmatrix} \hat{K} \ \hat{K}_v \end{bmatrix} G_{(y,v)v} = 0$$

that implies

$$\hat{K}_v = -\hat{K}G_{yv}.$$

Hence, the controller has the form (2.14). We now show that $\hat{K}$ is a stabilizing controller for G_{yu}. Consider

$$\hat{Q} := (I - \hat{K}G_{yu})^{-1}\hat{K}$$

and note that

$$\begin{aligned} Q &= (I - KG_{(y,v)u})^{-1}K \\ &= (I - \hat{K}G_{yu})^{-1}\hat{K}R \\ &= \hat{Q}[I \ \ -G_{yv}]. \end{aligned} \tag{2.16}$$

By multiplying $[I \ 0]^\mathsf{T}$ to (2.16) from the right side we have $\hat{Q} = Q[I \ 0]^\mathsf{T}$. From the assumption that $Q \in \mathcal{RH}_\infty$, $\hat{Q}$ belongs to $\mathcal{RH}_\infty$ as well. This leads to that $\hat{K}$ stabilizes G_{yu}.

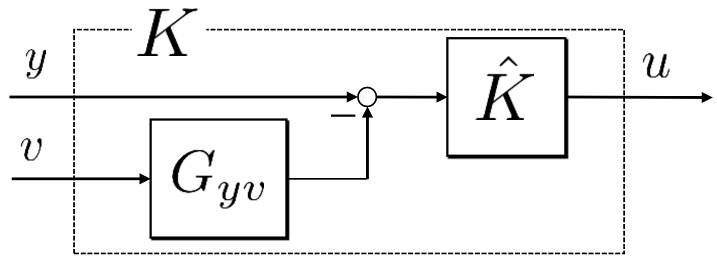

Fig. 2.5 Structure inside the output-rectifying retrofit controllers with the interconnection signal.

To prove the converse, we assume that the controller can be represented by (2.14) and $\hat{K}$ is a stabilizing controller for G_{yu}. Simple calculation leads to the condition (2.15) and the relationship (2.16) implies that Q belongs to $\mathcal{RH}_\infty$. Therefore, K is an output-rectifying retrofit controller. □

Theorem 3 indicates that all output-rectifying retrofit controllers with the interconnection signal from the environment hold the structure depicted by Fig. 2.5. If we implement $\hat{K}$ alone as a controller K, it is obvious that the entire system stability cannot be guaranteed since the measurement signal y is influenced by the interconnection signal v from the environment $G_{\rm E}$. The transfer matrix G_{yv} in Fig. 2.5 has the role to simulate the effect of the interconnection signal to the measurement signal. Theorem 3 also implies that by placing the output rectifier $G_{\rm R}$ inside the retrofit controller we can produce the rectified measurement signal $y - G_{yv}v = G_{\rm R}[y^{\sf T}\ v^{\sf T}]^{\sf T}$ and stabilize the entire interconnected system using $\hat{K}$ and also this procedure is the only means to cope with all possible environments. Furthermore, Theorem 3 claims that all output-rectifying retrofit controllers can be parameterized with a local stabilizing controller $\hat{K}$ when the interconnection signal can be fed back. Thus the new design parameter $\hat{Q}$ can be taken as any element in $\mathcal{RH}_\infty$. It should be emphasized that the structure in Fig. 2.5 is the exactly same as that introduced in the existing study [19], in which it is shown that controllers that have the structure become a retrofit controller, that is, the structure is a sufficient condition for retrofit control.

To discuss control performance, we explicitly give the closed-loop map when the controller is an output-rectifying retrofit controller with the interconnection measurement. The following theorem holds.

Theorem 4 *If K is an output-rectifying retrofit controller with the interconnection signal, then the closed-loop map from d to z can be represented by*

$$T_{\rm all} = \hat{T}_{zd}(\hat{Q}) + G_{zv} Q_{\rm E} \hat{T}_{wd}(\hat{Q}),$$

where

$$\hat{T}_{zd}(\hat{Q}) := G_{zd} + G_{zu}\hat{Q}G_{yd}, \quad \hat{T}_{wd}(\hat{Q}) := G_{wd} + G_{wu}\hat{Q}G_{yd}.$$

Proof: From Theorem 2, the closed-loop map can be represented by (2.9). Since

$$\begin{aligned} QG_{(y,v)d} &= Q \begin{bmatrix} G_{yd} \\ 0 \end{bmatrix} \\ &= \hat{Q}G_{\rm R} \begin{bmatrix} G_{yd} \\ 0 \end{bmatrix} \\ &= \hat{Q}G_{yd}, \end{aligned}$$

we have $T_{zd}(Q) = \hat{T}_{zd}(\hat{Q})$ and $T_{wu}(\hat{Q}) = \hat{T}_{wu}(\hat{Q})$. Moreover, the condition (2.15) leads to that $T_{zv}(Q) = G_{zv}$. Substituting these relationships to (2.9) yields the claim. □

Theorem 4 implies that not only the closed-loop map is an affine function with respect to $Q_{\rm E}$ but also the transfer matrices $\hat{T}_{zd}$ and $\hat{T}_{wu}$ are affine functions with respect to the design parameter $\hat{Q}$ as well. It should be emphasized that the design parameter in Theorem 4 is represented by $\hat{Q}$ that is unconstrained in contrast to the case of Theorem 2. Theorem 4 also implies that the effects from the external disturbance d to the evaluated output z and the interconnection signal w should be suppressed simultaneously when the model information on $Q_{\rm E}$ is unknown. In summary, the result suggests that for a retrofit controller design problem we only have to solve an unconstrained convex optimization problem where the design parameter is $\hat{Q}$ that suppresses both $\hat{T}_{zd}$ and $\hat{T}_{wd}$ and construct the associated output-rectifying retrofit controller according to the structure in Fig. 2.5 using the corresponding $\hat{K}$. The block diagram of the closed-loop map is illustrated by Fig. 2.6.

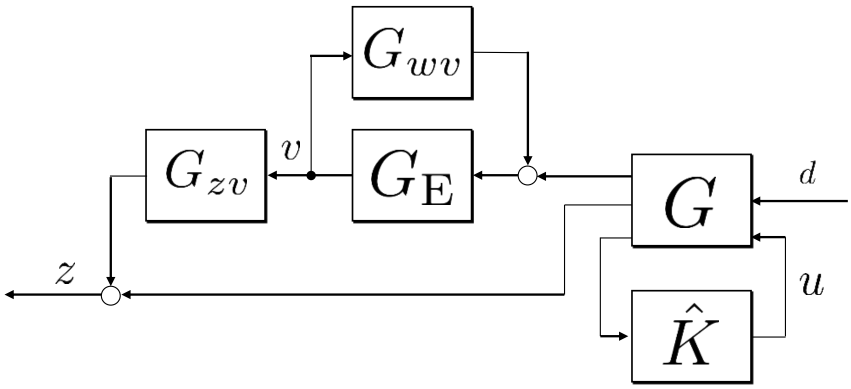

Fig. 2.6 Block diagram of the closed-loop map with an output-rectifying retrofit controller.

2.5 Dual Results in Input-Rectifying Retrofit Controllers

In this subsection, we focus on input-rectifying retrofit controllers and derive dual results that correspond to the theorems shown in the previous section. It is revealed that all input-rectifying retrofit controllers can be parameterized with an unconstrained design parameter under dual assumptions as with the case of output-rectifying retrofit controllers.

While we have considered the case in which the interconnection signal v is available at K, we consider the case where control input can be directly injected into the interconnection signal w as a dual case; that is, the control input can be represented by

$$\begin{bmatrix} u \\ u_w \end{bmatrix} = Ky \tag{2.17}$$

and the interconnection signal w can be represented by

$$w = G_{wv}v + G_{wd}d + G_{wu}u + u_w. \tag{2.18}$$

It is shown that all input rectifying retrofit controllers can be parameterized with a local stabilizing controller and have a dual structure under the assumption as with output-rectifying retrofit controllers.

The following theorem holds.

Theorem 5 *Assume that the control input and the interconnection signal can be represented by* (2.17) *and* (2.18)*, respectively. Then K is an input-rectifying retrofit controller if and only if the controller has the form*

$$K = G_{\rm R}^{\rm d}\hat{K},$$

where $\hat{K}$ is a controller that stabilizes G_{yu} with

$$G_{\rm R}^{\rm d} := \begin{bmatrix} I \\ -G_{wu} \end{bmatrix}.$$

Furthermore, the closed-loop map with an input-rectifying retrofit controller can be represented by

$$T_{\rm all} = \hat{T}_{zd}^{\rm d}(\hat{Q}) + \hat{T}_{zv}^{\rm d}(\hat{Q})Q_{\rm E}G_{wd},$$

where

$$\hat{T}_{zd}^{\rm d}(\hat{Q}) := G_{zd} + G_{zu}\hat{Q}G_{yd}, \quad \hat{T}_{zv}^{\rm d}(\hat{Q}) := G_{zv} + G_{zu}\hat{Q}G_{yv},$$

with $\hat{Q} := \hat{K}(I - G_{yu}\hat{K})^{-1}$.

Proof: Assume that $Q \in \mathcal{RH}_\infty$ and the condition (2.12) is satisfied. Suppose

$$\begin{bmatrix} u \\ u_w \end{bmatrix} = \begin{bmatrix} \hat{K} \\ \hat{K}_w \end{bmatrix} y,$$

with transfer matrices $\hat{K}$ and $\hat{K}_w$. Note that the condition (2.12) is written by

$$[G_{wu}\ I]\begin{bmatrix} \hat{K} \\ \hat{K}_w \end{bmatrix} = 0,$$

in this case. Then the condition (2.12) implies that

$$\hat{K}_w = -G_{wu}\hat{K},$$

and hence the controller can be represented by (2.17). Now we show that $\hat{K}$ is a stabilizing controller for G_{yu}. Consider $\hat{Q} := \hat{K}(I - G_{yu}\hat{K})^{-1}$ and

$$Q = G_{\rm R}^{\rm d}\hat{Q}.$$

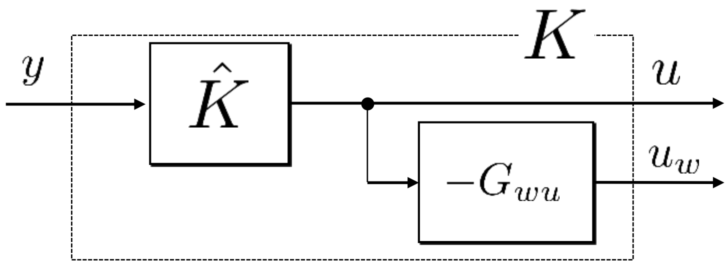

Fig. 2.7 Structure inside the input-rectifying retrofit controllers under full-control for the interconnection signal.

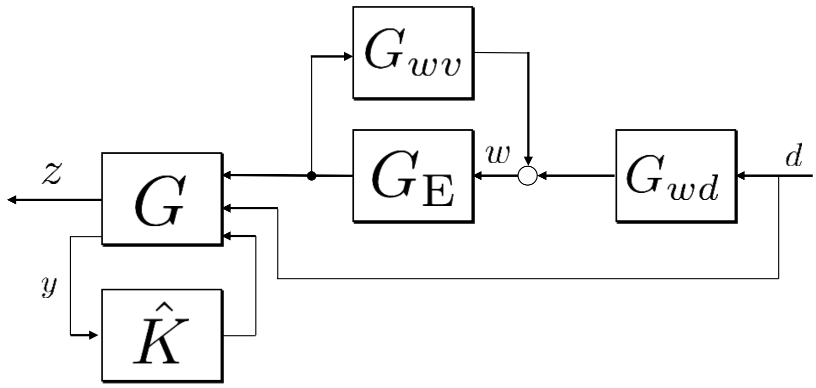

Fig. 2.8 Block diagram of the closed-loop map with an input-rectifying retrofit controller.

By multiplying $[I\ 0]$ from the left side we obtain the conclusion. Finally, simple calculation leads to the closed-loop map as with Theorem 4. □

Theorem 5 indicates that all input-rectifying retrofit controllers under the assumption hold the structure depicted by Fig. 2.7. The structure can be regarded as a dual one in Fig. 2.5. While the output rectifier in Fig. 2.5 has the role to rectify the measurement output, the input rectifier $G_{\mathrm{R}}^{\mathrm{d}}$ has the role to rectify the control input. According to Theorem 5, as with the case of the output rectifying retrofit controllers, the structure in Fig. 2.7 is a necessary and sufficient condition for guaranteeing the stability for any possible environment. Moreover, the degree of freedom of the controller design is expressed by $\hat{K}$ that stabilizes G_{yu} in this case as well. The block diagram of the closed-loop map is illustrated by Fig. 2.8.

2.6 Chapter Summary

In this chapter, we have proposed a novel retrofit control approach for distributed design of local controllers. We have first introduced the definition of retrofit controllers and derived a necessary and sufficient condition to characterize retrofit controllers in the frequency domain using Youla parameterization. It has been seen that the retrofit controller design problem is rather difficult in the general situation. To resolve this issue, two classes of retrofit controllers, output-rectifying retrofit controllers and input-rectifying retrofit controllers, have been defined. It has been reveled that all output-rectifying retrofit controllers can be parameterized under the assumption that the interconnection signal from the environment can be fed back and its design problem is much easier than the general case. Moreover, dual results in input-rectifying retrofit controllers have been shown. These results enable us to design local controllers for a large-scale dynamical network system in a distributed manner.

Although the results establish a fundamental theory for distributed design based on retrofit control, there remain several issues to be resolved. First, the assumption on the measurability of the interconnection signal is required in theory but this assumption is not always satisfied. The second issue is that the effectiveness has not been verified in practical systems yet. Finally, the information structure of the designed controllers are purely decentralized. The aim of the following chapters is to resolve these issues.

Chapter 3

Output-Rectifying Retrofit Controllers without Interconnection Signal

3.1 Introduction

Our aim in this chapter is to develop a design method of output-rectifying retrofit controllers without interconnection signal. In practical network systems, it is desirable to design a retrofit controller without interconnection signal because implementing sensors to obtain the interconnection signal often costs and it is sometimes impossible to measure the interconnection signal. For ease of discussion, we consider state-feedback output-rectifying retrofit controllers and show that a similar parameterization to that in the previous chapter is available in this case as well.

This chapter is organized as follows. In Section 3.2, we provide the system model treated in this chapter and consider the design problem of a state-feedback output-rectifying retrofit controller. Section 3.3 gives a parameterization of all state-feedback output-rectifying retrofit controllers and proposes a design method. Finally, Section 3.5 concludes this chapter.

3.2 System Model

In this chapter, we consider linear time-invariant interconnected systems (2.1) and assume that the state-space representation of G is given by

$$G : \begin{cases} \dot{x} &= Ax + Lv + Rd + Bu \\ w &= \Gamma x \\ z &= Sx \\ y &= x \end{cases} \tag{3.1}$$

where x is the state of G. Without loss of generality, we assume that L and B are full-column rank matrices. In the state-space representation, feedthrough terms are omitted for simplicity. Our purpose is to suppress the effect from d to z by designing a retrofit controller K for

$$u = Kx \tag{3.2}$$

without the interconnection signal v.

In the previous chapter, we have observed that all output-rectifying retrofit controllers can be represented with an unconstrained design parameter when the interconnection signal is measurable. In this chapter we attempt to relax this assumption. It will be shown that all state-feedback output rectifying retrofit controllers have a structure similar to that in Fig. 2.5.

3.3 Parameterization of All State-Feedback Output-Rectifying Retrofit Controllers

This section gives a parameterization of all state-feedback output-rectifying retrofit controllers. The basic idea for synthesizing a state-feedback retrofit controller is explained as follows [19]. For P being a full-row rank matrix such that

$$\operatorname{im} L \subset \ker P, \tag{3.3}$$

we consider applying the basis transformation of

$$x = P^{\dagger}\phi + \overline{P}^{\dagger}\overline{\phi}$$

with

$$\phi := Px, \quad \overline{\phi} := \overline{P}x$$

where $\overline{P}$ is a matrix that satisfies the relationship $P^\dagger P + \overline{P}^\dagger \overline{P} = I$. Then the dynamics with respect to ϕ can be described as

$$\begin{aligned}\dot{\phi} &= PAP^\dagger \phi + PA\overline{P}^\dagger \overline{\phi} + PLv + PRd + PBu \\ &= PAP^\dagger \phi + PA\overline{P}^\dagger \overline{\phi} + PRd + PBu.\end{aligned} \tag{3.4}$$

The key observation here is that L is eliminated in (3.4) owing to the condition (3.3). By regarding ϕ and $\overline{\phi}$ as a new measurement signal and a virtual interconnection signal, respectively, we can construct a retrofit controller for the reduced-order model (3.3) based on the structure in Chapter 2. Note that the above procedure gives a sufficient structure of state-feedback retrofit controllers, but does not claim any necessity of the controller structure.

The following theorem shows that all state-feedback output-rectifying retrofit controllers without interconnection signal are necessarily synthesized by such a procedure.

Theorem 6 *The controller K in* (3.2) *is a state-feedback output-rectifying retrofit controller without interconnection signal if and only if the controller can be represented by*

$$K = \hat{K}\tilde{G}_{\mathrm{R}} \tag{3.5}$$

where $\hat{K}$ is a controller that stabilizes

$$G_{\phi u} := (sI - PAP^\dagger)^{-1}PB$$

and P is a full-row rank matrix such that the condition

$$\operatorname{im} L = \ker P \tag{3.6}$$

holds with

$$\tilde{G}_{\mathrm{R}} := P - (sI - PAP^\dagger)^{-1}PA\overline{P}^\dagger \overline{P}.$$

Proof: The proof is built on two parts. In the former part, we prove that all retrofit controllers have the form (3.5). In the later part, we prove that $\hat{K}$ belongs to the class of controllers that stabilize $G_{\phi u}$.

In the former part, we show that all solutions in $\mathcal{RP}$ to the equation (2.11) is represented as the form (3.5), or equivalently,

$$KG_{yv} = 0 \Leftrightarrow {}^\exists \hat{K} \in \mathcal{RP} \text{ s.t. } K = \hat{K}\tilde{G}_{\mathrm{R}}. \tag{3.7}$$

Note that $G_{yu} = (sI - A)^{-1}L$ in this chapter.

As a preparation, we give all solutions in $\mathcal{R}$ to the equation (2.11). Now let n be the dimensions of x. Because $\mathcal{R}$ is a vector space, the fundamental theorem on homomorphisms leads to that for $K \in \mathcal{R}$

$$KG_{yv} = 0 \Leftrightarrow {}^{\exists}\hat{K} \in \mathcal{R} \text{ s.t. } K = \hat{K}\Xi \tag{3.8}$$

for any transfer matrix Ξ that is an element in $\mathcal{R}$ and satisfies the conditions

$$\dim(\operatorname{im}\Xi) = n - \dim(\operatorname{im}G_{yv}) \tag{3.9}$$

and

$$\ker\Xi = \operatorname{im}G_{yv} \subset \mathcal{R}^n. \tag{3.10}$$

We now take

$$\Xi := P\{I - (sI - A)^{-1}LL^{\dagger}(sI - A)\} \in \mathcal{R}. \tag{3.11}$$

Let us confirm that the above transfer matrix satisfies the conditions. By checking the feedthrough term of Ξ, we have

$$\lim_{s\to\infty}\Xi(s) = P(I - LL^{\dagger})$$

and $\Xi \in \mathcal{RP}$. Because

$$\begin{aligned}\operatorname{im}(I - LL^{\dagger}) &= (\operatorname{im}L)^{\perp}\\ &= (\ker P)^{\perp}\end{aligned}$$

from the condition (3.6), $P(I - LL^{\dagger})$ is full-row rank. Since Ξ belongs to $\mathcal{RP}$ and its feedthrough term is right-invertible, Ξ is right-invertible in $\mathcal{RP}$. Hence,

$$\dim(\operatorname{im}\Xi) = \dim(\operatorname{im}P)$$

and Ξ satisfies the condition (3.9). Moreover, we have

$$\begin{aligned}\Xi G_{yv} &= P\{G_{yv} - (sI - A)^{-1}L\}\\ &= 0\end{aligned}$$

and thus Ξ satisfies the condition (3.10) as well. The above discussion implies that, for such Ξ, if $K \in \mathcal{R}$ satisfies the condition in (3.8), there always exists $\hat{K} \in \mathcal{R}$ such that the condition in (3.8) is satisfied, and the converse holds as well.

Next, we show that K satisfying the condition in (3.8) for Ξ defined by (3.11) belongs to $\mathcal{RP}$ if and only if $\hat{K}$ belongs to $\mathcal{RP}$, or roughly, K is proper if and only if $\hat{K}$ is proper. From the relationship $K = \hat{K}\Xi$, it is obvious that if $\hat{K}$ is proper then K is proper. For the converse, we have $K\Xi^\dagger = \hat{K}$ by multiplying $\Xi^\dagger$. Because $\Xi^\dagger$ also belongs to $\mathcal{RP}$, if K is proper then $\hat{K}$ is proper. Thus we see that for $K \in \mathcal{RP}$

$$KG_{yv} = 0 \Leftrightarrow {}^\exists \hat{K} \in \mathcal{RP} \text{ s.t. } K = \hat{K}\Xi.$$

We finally show that $\Xi = \tilde{G}_{\mathrm{R}}$. We have

$$\begin{aligned}\Xi &= P[I - (sI - A)^{-1}Ls\{(sI - A)^{-1}Ls\}^\dagger] \\ &= P\left(I - \left[\begin{array}{c|c} A & AL \\ \hline I & L \end{array}\right]\left[\begin{array}{c|c} A - ALL^\dagger & ALL^\dagger \\ \hline -L^\dagger & L^\dagger \end{array}\right]\right)\end{aligned}$$

because

$$\left[\begin{array}{c|c} A & B \\ \hline C & D \end{array}\right]^\dagger = \left[\begin{array}{c|c} A - BD^\dagger C & BD^\dagger \\ \hline -D^\dagger C & D^\dagger \end{array}\right]$$

provided that D is left-invertible. Since

$$\left[\begin{array}{c|c} A_2 & B_2 \\ \hline C_2 & D_2 \end{array}\right]\left[\begin{array}{c|c} A_1 & B_1 \\ \hline C_1 & D_1 \end{array}\right] = \left[\begin{array}{cc|c} A_1 & 0 & B_1 \\ B_2C_1 & A_2 & B_2D_1 \\ \hline D_2C_1 & C_2 & D_2D_1 \end{array}\right],$$

we have

$$\Xi = P\left(I - \left[\begin{array}{cc|c} A\overline{LL}^\dagger & 0 & ALL^\dagger \\ -ALL^\dagger & A & ALL^\dagger \\ \hline -LL^\dagger & I & LL^\dagger \end{array}\right]\right).$$

By considering the coordinate transformation

$$\begin{bmatrix} I & -I \\ 0 & I \end{bmatrix}$$

we obtain

$$\left[\begin{array}{cc|c} A\overline{LL}^{\dagger} & 0 & ALL^{\dagger} \\ -ALL^{\dagger} & A & ALL^{\dagger} \\ \hline -LL^{\dagger} & I & LL^{\dagger} \end{array}\right] = \left[\begin{array}{cc|c} A & 0 & 0 \\ -ALL^{\dagger} & A\overline{LL}^{\dagger} & ALL^{\dagger} \\ \hline -LL^{\dagger} & I - LL^{\dagger} & LL^{\dagger} \end{array}\right]$$
$$= \left[\begin{array}{c|c} A\overline{LL}^{\dagger} & ALL^{\dagger} \\ \hline \overline{LL}^{\dagger} & LL^{\dagger} \end{array}\right].$$

Again, considering the coordinate transformation

$$\begin{bmatrix} \overline{P} \\ P \end{bmatrix},$$

we have

$$\left[\begin{array}{c|c} A\overline{LL}^{\dagger} & ALL^{\dagger} \\ \hline \overline{LL}^{\dagger} & LL^{\dagger} \end{array}\right] = \left[\begin{array}{cc|c} 0 & \overline{P}AP^{\dagger} & \overline{P}ALL^{\dagger} \\ 0 & PAP^{\dagger} & PALL^{\dagger} \\ \hline 0 & \overline{L} & LL^{\dagger} \end{array}\right]$$
$$= \left[\begin{array}{c|c} PAP^{\dagger} & PALL^{\dagger} \\ \hline \overline{L} & LL^{\dagger} \end{array}\right]$$

and hence

$$\Xi = \left[\begin{array}{c|c} PAP^{\dagger} & PA\overline{P}^{\dagger}\overline{P} \\ \hline -I & P^{\dagger} \end{array}\right]$$
$$= \tilde{G}_{\mathrm{R}}.$$

Therefore, it turns out that (3.7) holds.

In the later part, we show that K is a retrofit controller if and only if $\hat{K}$ in (3.7) belongs to the class of controllers that stabilize $G_{\phi u}$. For simplicity of discussion, we assume that

$$G_{\phi u} \in \mathcal{RH}_{\infty}.$$

Then what we have to show is written as

$$Q \in \mathcal{RH}_{\infty} \Leftrightarrow \hat{Q} \in \mathcal{RH}_{\infty}$$

where $\hat{Q} := (I - \hat{K}G_{\phi u})^{-1}\hat{K}$.

Now we have

$$
\begin{aligned}
\tilde{G}_{\mathrm{R}} G_{yu} &= \left[\begin{array}{c|c} PAP^{\dagger} & PA\overline{P}^{\dagger}\overline{P} \\ \hline -I & P^{\dagger} \end{array}\right] \left[\begin{array}{c|c} A & B \\ \hline I & 0 \end{array}\right] \\
&= \left[\begin{array}{cc|c} A & 0 & B \\ PA\overline{P}^{\dagger}\overline{P} & PAP^{\dagger} & 0 \\ \hline P^{\dagger} & -I & 0 \end{array}\right] \\
&= \left[\begin{array}{cc|c} A & 0 & B \\ 0 & PAP^{\dagger} & -PB \\ \hline 0 & -I & 0 \end{array}\right] \\
&= \left[\begin{array}{c|c} PAP^{\dagger} & PB \\ \hline I & 0 \end{array}\right] \\
&= G_{\phi u}
\end{aligned}
$$

with the coordinate transformation

$$
\begin{bmatrix} I & 0 \\ -P & I \end{bmatrix}.
$$

Therefore

$$
\begin{aligned}
Q &= (I - \hat{K}\tilde{G}_{\mathrm{R}} G_{yu})^{-1} \hat{K}\tilde{G}_{\mathrm{R}} \\
&= (I - \hat{K} G_{\phi u})^{-1} \hat{K}\tilde{G}_{\mathrm{R}} \\
&= \hat{Q}\tilde{G}_{\mathrm{R}}.
\end{aligned}
$$

From the assumption that $G_{\phi u} \in \mathcal{RH}_\infty$, $\tilde{G}_{\mathrm{R}}$ also belongs to $\mathcal{RH}_\infty$. Thus if $\hat{Q} \in \mathcal{RH}_\infty$ then $Q \in \mathcal{RH}_\infty$. Furthermore, since $\tilde{G}_{\mathrm{R}}$ is right-invertible, we have

$$
Q\tilde{G}_{\mathrm{R}}^{\dagger} = \hat{Q}.
$$

Because

$$
\tilde{G}_{\mathrm{R}}^{\dagger} = \left[\begin{array}{c|c} A & \overline{P}^{\dagger}\overline{P}AP^{\dagger} \\ \hline I & P^{\dagger} \end{array}\right],
$$

$\tilde{G}_{\mathrm{R}}^{\dagger} \in \mathcal{RH}_\infty$. Hence, if $Q \in \mathcal{RH}_\infty$ then $\hat{Q} \in \mathcal{RH}_\infty$. $\square$.

Theorem 6 implies that all state-feedback output-rectifying retrofit controllers can be parameterized with $\hat{K}$ that stabilizes the reduced-order model $G_{\phi u}$ and have the

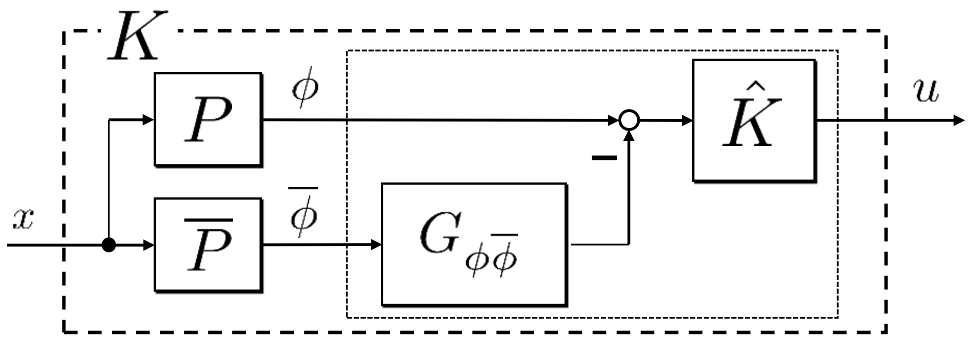

Fig. 3.1 Structure inside the state-feedback output-rectifying retrofit controllers where $G_{\phi\overline{\phi}}$ is defined by (3.16).

structure depicted by Fig. 3.1 with

$$G_{\phi\overline{\phi}} := (sI - PAP^{\dagger})^{-1}PA\overline{P}^{\dagger}. \tag{3.12}$$

It should be noted that the same structure in Fig. 2.5 can be observed in Fig. 3.1. Specifically, y, v and G_{yv} in Fig. 2.5 correspond to $\phi, \overline{\phi}$, and $G_{\phi\overline{\phi}}$, respectively. Note also that the proof cannot be directly extended to output feedback retrofit controllers because it is difficult to find a basis of $(\operatorname{im} G_{yv})^{\perp}$ in the output feedback setting while $\tilde{G}_{\mathrm{R}}$ is the basis for the state-feedback case.

The closed-loop map from d to z with a state-feedback retrofit controller can be represented with an unconstrained design parameter as well. The following theorem holds.

Theorem 7 *If K is a state-feedback output-rectifying retrofit controller, then the closed-loop map from d to z can be represented by*

$$T_{\mathrm{all}} = \tilde{T}_{zd}(\hat{Q}) + G_{zv}Q_{\mathrm{E}}\tilde{T}_{wu}(\hat{Q})$$

where

$$\tilde{T}_{zd}(\hat{Q}) := G_{zd} + G_{zu}\hat{Q}\hat{G}_{xd}, \quad \tilde{T}_{wu}(\hat{Q}) := G_{wd} + G_{wu}\hat{Q}\hat{G}_{xd}$$

with

$$\hat{G}_{xd} := (sI - PAP^{\dagger})^{-1}PR, \quad \hat{Q} := (I - \hat{K}G_{\phi u})^{-1}\hat{K}.$$

Proof: Because

$$G_{\phi u} = \tilde{G}_{\mathrm{R}}G_{xd}, \quad \hat{G}_{xd} = \hat{G}_{\mathrm{R}}G_{xd},$$

we have

$$\begin{aligned} QG_{xd} &= (I - \hat{K}\tilde{G}_{\mathrm{R}}G_{xu})^{-1}\hat{K}\tilde{G}_{\mathrm{R}}G_{xd} \\ &= \hat{Q}\hat{G}_{xd}. \end{aligned}$$

Therefore, as with the proof of Theorem 3, the claim holds. □

The transfer matrices $\tilde{T}_{zd}$ and $\tilde{T}_{wu}$ in Theorem 7 are affine functions with respect to the free design parameter $\hat{Q}$ as in Theorem 3. Thus the design problem of state-feedback output-rectifying retrofit controllers can be treated as a standard unconstrained controller design problem.

3.4 Dual Results

In this section, we give dual results on input-rectifying retrofit controllers. The logic for the statements in this subsection is the same as that in the previous section. Consequently, concrete proofs are omitted here.

We consider the following system

$$G : \begin{cases} \dot{x} &= Ax + Lv + Rd + u \\ w &= \Gamma x \\ z &= Sx \\ y &= Cx \end{cases} \tag{3.13}$$

for the local system instead of (3.1). The difference of (3.13) from (3.1) is that the input matrix B is equal to the identify and the measurement signal is not the state x itself but Cx. We place an assumption that Γ and C are full-row rank matrices. The controller is given by

$$u = Ky. \tag{3.14}$$

As a dual result of Theorem thmc3:str, a parameterization of input-rectifying retrofit controllers is given by

$$K = \tilde{G}_{\mathrm{R}}^{\mathrm{d}}\hat{K}$$

where K is a controller that stabilizes

$$G_{yu}^{\mathrm{d}} := CP(sI - P^{\dagger}AP)^{-1}$$

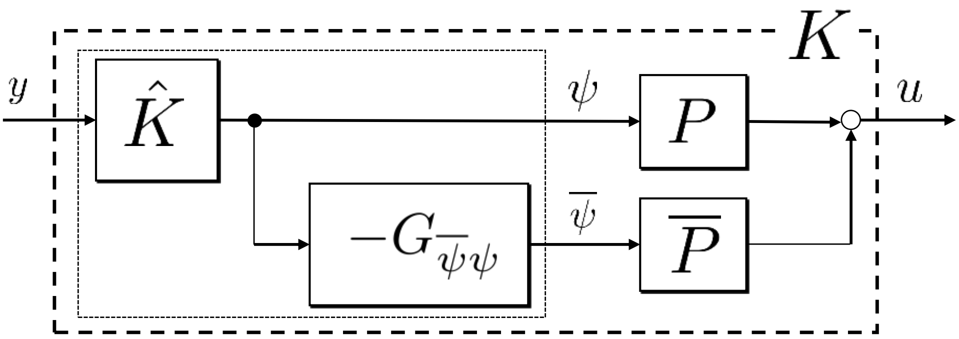

Fig. 3.2 Structure inside input-rectifying retrofit controllers where $\psi, \overline{\psi}$, and $G_{\overline{\psi}\psi}$ are defined by (3.15) and (3.16).

and P is a full-column rank matrix such that the condition

$$\ker \Gamma = \operatorname{im} P$$

holds with

$$\tilde{G}_{\mathrm{R}}^{\mathrm{d}} := P - \overline{P}\,\overline{P}^{\dagger} AP(sI - P^{\dagger}AP)^{-1}$$

As shown in Fig. 3.2, the dual structure can be observed in this case compared with Fig. 3.1 where ψ and $\overline{\psi}$ are defined by

$$u = P\psi + \overline{P\psi} \tag{3.15}$$

and

$$G_{\overline{\psi}\psi} := \overline{P}^{\dagger} AP(sI - P^{\dagger}AP)^{-1}. \tag{3.16}$$

Furthermore, the closed-loop map with an input-rectifying retrofit controller can be represented by

$$T_{\mathrm{all}} = \tilde{T}_{zd}^{\mathrm{d}}(\hat{Q}) + \tilde{T}_{zv}^{\mathrm{d}}(\hat{Q}) Q_{\mathrm{E}} G_{wd}$$

where

$$\tilde{T}_{zd}^{\mathrm{d}}(\hat{Q}) := G_{zd} + \hat{G}_{zu}\hat{Q}G_{yd}, \quad \tilde{T}_{wd}^{\mathrm{d}}(\hat{Q}) := G_{wd} + \hat{G}_{wu}\hat{Q}G_{yd},$$

with

$$\hat{G}_{zu} := S(sI - P^{\dagger}AP)^{-1}, \quad \hat{G}_{wu} := \Gamma(sI - P^{\dagger}AP)^{-1}.$$

For design of input-rectifying retrofit controllers, the same procedure can be performed as that for output-rectifying retrofit controllers.

3.5 Chapter Summary

In this chapter, we have considered design of retrofit controllers without interconnection signal and extend the result in Chapter 2. A parameterization of all state-feedback retrofit controllers has been derived. It has been also shown that a similar structure can be observed in state-feedback retrofit controllers to that of retrofit controllers with interconnection signal. Finally, we have seen that dual results can be obtained for input-rectifying retrofit controllers.

Chapter 4

Distributed Design of Power System Stabilizers in Power Grids with Renewable Energy Resources

4.1 Introduction

In this chapter, we consider the stabilization problem of power grids where a large amount of renewable energy resources is introduced. Many controller design methods have been proposed in the control community, but most of them require the entire system model and this assumption is not realistic as stated in Chapter 1. In contrast, distributed design has been practically employed for stabilizing controllers, e.g., PSSs. The typical distributed design method uses the single-machine infinite-bus system [21] that fucuses only on the dynamics of the subsystem of interest and ignores the other parts. As a result, assurance of the stability of the entire grid is not theoretically obtained. To resolve the issue, a novel distributed design method via retrofit control is proposed. The advantage of the proposed method is that theoretical guarantee of the stability of the entire grid is obtained.

We first review the importance of frequency control of power grids where a large amount of PV is penetrated. To develop sophisticated power grids, appropriate usage of renewable energy resources including PV plants plays an important role [30]. The feed-in tariff (FIT) [31] accelerates the progress of installing PV power generators and, as a result, the number of PV power plants in Japan is mounting up. The total quantity of installed PV generation is anticipated to reach 64 GW by 2030. It covers 7% of the total energy consumption approximately [32]. Due to the large installation of PV plants, some thermal power plants have to stop its operation for balancing the supply and demand since the demand is invariant though the amount of generated energy is increased by the installed PV plants. In [33–35], it has been pointed out that power grids tend to become unstable by stopping a number of synchronous generators due to the poor controllability of PV plants [36]. This poses the stabilization problem for future grids and a novel design method for PSSs that improve damping performance of power grids with PV plants while keeping the stability.

Distributed control [37–39] is a promising approach that fulfills the requirement. In distributed control, control inputs generated from local controllers depend only on the corresponding local measurement signal, e.g., deviation of the frequency of the associated synchronous generator. However, these distributed control methods are built on the premise that the system model of the whole power grid is utilizable for controller design. As noted above, since power grids are totally complex, the whole model is inaccessible. This fact leads to that these approaches are not very appropriate for practical power grids.

The aim of this chapter is to develop a distributed design method for PSSs based on retrofit control and to show how retrofit control works for the task. It is observed that the proposed method can significantly reduce the effect of disturbance injected into the power grid through a numerical simulation.

The organization of this chapter is as follows. We give a mathematical model of the power grids in Section 4.2. The PSS design problem is mathematically formulated in Section 4.3. Furthermore, a distributed design method for PSSs is proposed via retrofit control developed in the previous sections. For the purpose of demonstrating the efficiency of the approach, Section 4.4 shows a numerical simulation for PV-integrated IEEJ EAST 30-machine power system [25], called EAST30 model for short. Section 4.5 concludes this chapter.

4.2 Modeling of PV-Integrated Power Systems

First of all, we give a mathematical model of a power grid consisting of synchronous generators, loads, PV plants, and transmission lines of EAST30 model [25] in the state-space form. For giving a reasonable model, neighboring synchronous generators, loads, and PV plants are treated as aggregated ones. Buses have the role to interconnect the aggregated facilities. Throughout this thesis, we refer to the buses to which no facilities are not assigned as non-unit buses, and a facility connected to a bus or a non-unit bus as a component.

Let us suppose that there exist N buses in the power grid. Let $\mathbb{N} := \{1, \ldots, N\}$ and for $k \in \mathbb{N}$, the mathematical model of the kth component is given by

$$\Sigma_{[k]} : \begin{cases} \dot{x}_{[k]} &= f_{[k]}(x_{[k]}, \boldsymbol{v}_{[k]}, \boldsymbol{i}_{[k]}, u_{\mathrm{s},[k]}, u_{[k]}) \\ 0 &= g_{[k]}(x_{[k]}, \boldsymbol{v}_{[k]}, \boldsymbol{i}_{[k]}), \end{cases} \tag{4.1}$$

where $x_{[k]}$ is the state, $u_{\mathrm{s},[k]}$ is the supplementary control input, $u_{[k]}$ is the control input from the corresponding PSS, and $\boldsymbol{i}_{[k]}$ and $\boldsymbol{v}_{[k]}$ are the bus current and voltage, respectively.

The network structure of the grid is given by

$$\boldsymbol{i} = \boldsymbol{Y}\boldsymbol{v} \tag{4.2}$$

where

$$\boldsymbol{i} := \mathrm{col}(\boldsymbol{i}_{[k]})_{k\in\mathbb{N}}, \quad \boldsymbol{v} := \mathrm{col}(\boldsymbol{v}_{[k]})_{k\in\mathbb{N}}$$

and $\boldsymbol{Y} \in \mathbb{C}^{N\times N}$ is the admittance matrix. For the specific values of $\boldsymbol{Y}$ in the targeted power grid, see [40].

The model of the whole power grid can be obtained by combining (4.1) and (4.2). We give more detailed models of synchronous generators, loads, PV power plants, and non-unit buses as (4.1) In the following, the index set of the buses connecting to the generators, loads, PV power plants, and non-unit buses are defined by $\mathbb{N}_{\mathrm{G}}, \mathbb{N}_{\mathrm{L}}, \mathbb{N}_{\mathrm{P}}$ and $\mathbb{N}_{\mathrm{N}}$, respectively. Those sets are assumed to be disjoint and $\mathbb{N}_{\mathrm{G}} \cup \mathbb{N}_{\mathrm{L}} \cup \mathbb{N}_{\mathrm{P}} \cup \mathbb{N}_{\mathrm{N}} = \mathbb{N}$ holds.

4.2.1 Synchronous Generator

We give a model of synchronous generators that have the form (4.1). In a typical case, a synchronous generator is composed of a synchronous machine, an excitation system with automatic voltage regulator (AVR), and a turbine with governor [2]. The excitation system has the role to feed current to the synchronous machine. The turbine with governor rotates the machine by feeding a mechanical power. The synchronous machine converts the mechanical power to electrical power and provides the generated electrical power to the power system. For $k \in \mathbb{N}_{\mathrm{G}}$, the mathematical model of the synchronous machine associated with the kth bus is given by

$$\begin{cases} \dot{\delta}_{[k]} &= \bar{\omega}\omega_{[k]} \\ \dot{\omega}_{[k]} &= \dfrac{1}{M_{[k]}}\left(\dfrac{1}{1+\omega_{[k]}}P_{\mathrm{m},[k]} - v_{[k]}^{\mathsf{T}} i_{[k]}\right) \\ \Psi_{[k]} &= A_{\Psi[k]}\Psi_{[k]} + B_{\Psi[k]} i_{[k]} + B_{V[k]} V_{\mathrm{fd},[k]} \\ v_{[k]} &= C_{\Psi[k]}\Psi_{[k]} + D_{\Psi[k]} i_{[k]} \\ \boldsymbol{v}_{[k]} &= \mathbf{comp}(T_{\delta[k]} v_{[k]}) \\ \boldsymbol{i}_{[k]} &= \mathbf{comp}(T_{\delta[k]}^{-1} i_{[k]}) \end{cases}, \quad k \in \mathbb{N}_{\mathrm{G}} \tag{4.3}$$

where $\delta_{[k]}$ denotes the rotor angle relative to the frame rotating at the constant reference speed $\bar{\omega} := 100\pi$ (rad/sec), $\omega_{[k]}$ denotes the rotor angular velocity relative to $\bar{\omega}$, $\Psi_{[k]}$ includes the magnetic flux associated with the field circuit, d-axis damper windings, q-axis damper windings, $P_{\mathrm{m},[k]}$ denotes the mechanical power input, $V_{\mathrm{fd},[k]}$ denotes the field voltage, and $i_{[k]}$ and $v_{[k]}$ denote the stator current and the stator voltage, respectively. The inertia constant is represented by $M_{[k]}$ (sec) and $T_{\delta[k]}$ is given by

$$T_{\delta[k]} := \begin{bmatrix} \sin\delta_{[k]} & \cos\delta_{[k]} \\ -\cos\delta_{[k]} & \sin\delta_{[k]} \end{bmatrix}$$

that is the coordinate transformation matrix from the coordinate system rotating at each generator's own frequency to the coordinate system rotating at the rated frequency. It should be noted that the system (4.3) is related to the coordinate system that rotates at the rotational speed $\omega_{[k]}$.

The model of the turbine with governor is given by

$$\begin{cases} \dot{\zeta}_{[k]} &= A_{\zeta[k]}\zeta_{[k]} + B_{\zeta[k]}\omega_{[k]} + R_{\zeta[k]}(P_{\mathrm{m},[k]}^{\star} + u_{\mathrm{s},[k]}) \\ P_{\mathrm{m},[k]} &= C_{\zeta[k]}\zeta_{[k]} \end{cases} \tag{4.4}$$

where $\zeta_{[k]} \in \mathbb{R}^4$ denotes the state of the turbine with governor, $P_{\mathrm{m},[k]}^{\star}$ denotes the mechanical power in the steady state, and $u_{\mathrm{s},[k]}$ is the supplementary generation control action under automatic generation control (AGC) [2]. AGC has the role to regulate frequency to a pre-defined setpoint. The measurement signal of the supplementary generation control is given by aggregating all frequency deviations [2] and the control input is given by

$$u_{\mathrm{s},[k]}(t) = \kappa_{\mathrm{s}} a_{[k]} \int_0^t \sum_{k\in\mathbb{N}_{\mathrm{G}}} \omega_{[k]}(\tau) d\tau \tag{4.5}$$

where κ_s is a feedback gain, $a_{[k]}$ is a scaling factor, and the aggregated frequency deviation $\sum_{k\in\mathbb{N}_\mathrm{G}}\omega_{[k]}$ is referred to as an area control error. Moreover, it is supposed that the parameters in (4.5) are given so as to stabilize the entire system for the situation $u_{[k]}=0$.

The dynamics of the excitation system with AVR is represented as

$$\begin{cases} \dot{\eta}_{[k]} &= A_{\eta[k]}\eta_{[k]} + B_{\eta[k]}\left(\|v^\star_{[k]}\| - \|v_{[k]}\| + u_{[k]}\right) + R_{\eta[k]}V^\star_{\mathrm{fd},[k]} \\ V_{\mathrm{fd},[k]} &= C_{\eta[k]}\eta_{[k]} \end{cases} \tag{4.6}$$

where $\eta_{[k]}\in\mathbb{R}^3$ denotes the state of the excitation system with AVR, $\boldsymbol{v}^*_{[k]}$ denots the steady voltage, $V_{\mathrm{fd},[k]}$ denotes the steady field voltage, and $u_{[k]}$ denotes the control input from PSS. The excitation system with AVR has the function providing current to the synchronous machine.

The model of the synchronous generator is given as the combination of (4.3), (4.4), and (4.6). The state of a synchronous generator is defined by

$$x_{[k]} := \mathrm{col}(\delta_{[k]}, \omega_{[k]}, \Psi_{[k]}, \zeta_{[k]}, \eta_{[k]}) \in \mathbb{R}^{13}, \quad k\in\mathbb{N}_\mathrm{G}$$

and $f_{[k]}(\cdot,\cdot)$ and $g_{[k]}(\cdot,\cdot)$ obey (4.3), (4.4), and (4.6). Fig. 4.1 depicts the block diagram of the model of the synchronous generator. The measurement output is given by

$$y_{[k]} := \mathrm{col}(\omega_{[k]}, v_{[k]})$$

for each generator.

The specific values of the parameters of synchronous generators are given as follows. There exist three sorts of generator, that is, thermal power plants, nuclear power plants, and hydroelectric power plants, in the power system considered in this thesis. For simplicity, the subscript $k\in\mathbb{N}_\mathrm{G}$ is omitted. The matrices of the synchronous machine in (4.3) are

$$A_\Psi = \begin{bmatrix} \dfrac{-(1+\gamma_d)}{T'_{do}} & \dfrac{K_d\gamma_d}{T'_{do}} & 0 & 0 \\ \dfrac{1}{K_dT''_{do}} & \dfrac{-1}{T''_{do}} & 0 & 0 \\ 0 & 0 & \dfrac{-(1+\gamma_q)}{T'_{qo}} & \dfrac{K_q\gamma_q}{T'_{qo}} \\ 0 & 0 & \dfrac{1}{K_qT''_{qo}} & \dfrac{-1}{T''_{qo}} \end{bmatrix},$$

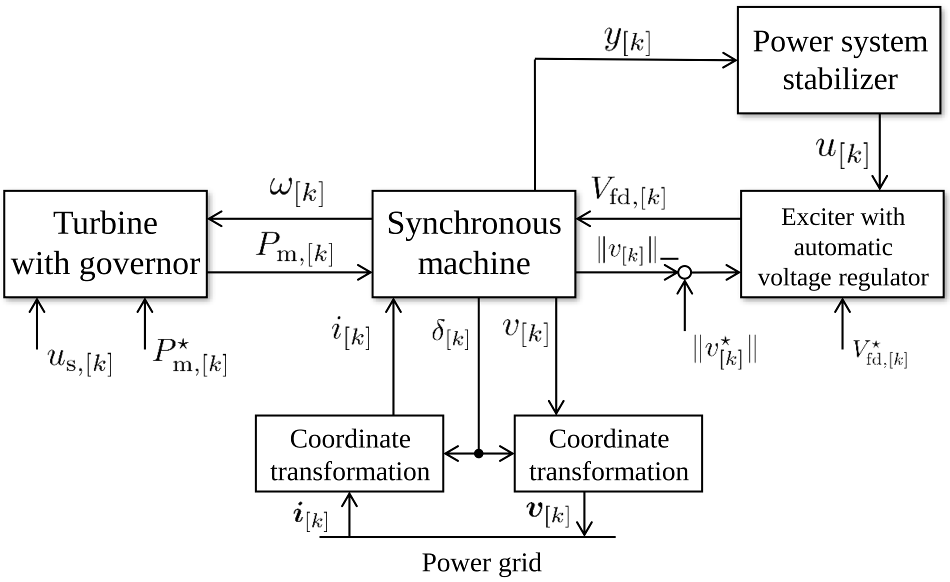

Fig. 4.1 Block diagram of the model of the generator.

$$
\begin{aligned}
B_\Psi &= \begin{bmatrix} -\dfrac{(X_d - X_d')(X_d'' - X_l)}{T_{do}'(X_d' - X_l)} & 0 \\ -\dfrac{X_d' - X_l}{K_d T_{do}''} & 0 \\ 0 & \dfrac{(X_q - X_q')(X_q'' - X_l)}{T_{qo}'(X_q' - X_l)} \\ 0 & \dfrac{X_q' - X_l}{K_q T_{qo}''} \end{bmatrix}, \\
B_V &= [1/T_{do}' \ 0 \ 0 \ 0]^\mathsf{T} \\
C_\Psi &= \begin{bmatrix} 0 & 0 & \dfrac{X_q'' - X_l}{X_q' - X_l} & K_q \dfrac{X_q' - X_q''}{X_q' - X_l} \\ \dfrac{X_d'' - X_l}{X_d' - X_l} & K_d \dfrac{X_d' - X''}{X_d' - X_l} & 0 & 0 \end{bmatrix}, \\
D_\Psi &= \begin{bmatrix} 0 & X_q'' \\ -X_d'' & 0 \end{bmatrix},
\end{aligned}
$$

$$\gamma_\circ := \frac{(X_\circ - X'_\circ)(X'_\circ - X''_\circ)}{(X'_\circ - X_l)^2},$$
$$K_\circ := 1 + \frac{(X'_\circ - X_l)(X''_\circ - X_l)}{(X'_\circ - X''_\circ)(X_\circ - X_l)}, \quad \circ \in \{d, q\},$$

where $X_d, X'_d, X''_d, T'_{do}, T''_{do}$ denote d-axis synchronous reactance, transient reactance, subtransient reactance, and transient open-circuit, $X_q, X'_q, X''_q, T'_{qo}, T''_{qo}$ denote similar q-axis quantities, and X_l denote a stator leakage reactance (for the specific values, see [40]). It should be noted that the parameters of the synchronous machine are exactly the same for all sorts of generators. The matrices of the turbine with governor in (4.4) for thermal power plants and nuclear power plants are given as

$$A_\zeta = \begin{bmatrix} -5 & 0 & 0 & 0 \\ -5 & -5 & 0 & 0 \\ 0 & 4 & -4 & 0 \\ 0 & 0 & \frac{1}{9} & -\frac{1}{9} \end{bmatrix}, \quad B_\zeta = \begin{bmatrix} 125 \\ 0 \\ 0 \\ 0 \end{bmatrix},$$
$$R_\zeta = [0\ 5\ 0\ 0]^\mathsf{T}, \quad C_\zeta = [0\ 0\ 0.3\ 0.7].$$

The matrices for hydroelectric power plants is given by

$$A_\zeta = \begin{bmatrix} -0.01 & -0.25 & 0 & 0 \\ -\frac{1}{2000} & -\frac{2.3}{24} & 0 & 0 \\ \frac{1}{7} & 0 & -\frac{1}{7} & 0 \\ 0 & 0 & \frac{2}{3} & -\frac{2}{3} \end{bmatrix}, \quad B_\zeta = \begin{bmatrix} -0.25 \\ -\frac{1}{80} \\ 0 \\ 0 \end{bmatrix},$$
$$R_\zeta = \left[0\ 0\ \frac{1}{7}\ 0\right]^\mathsf{T}, \quad C_\zeta = [0\ 0\ -2\ 3].$$

The matrices for the excitation system with AVR in (4.6) are given as

$$A_\eta = \begin{bmatrix} -5 & 0 & -5 \\ 50 & -0.5 & 0 \\ 10 & -0.1 & -2 \end{bmatrix}, \quad B_\eta = \begin{bmatrix} 5 \\ 0 \\ 0 \end{bmatrix}, \quad R_\eta = [0\ 0.5\ 0.1]^\mathsf{T}, \quad C_\eta = [0\ 1\ 0].$$

It should be noted that all sorts of synchronous generator have the same parameters with respect to the excitation system as synchronous machine.

4.2.2 Load, PV Power Plant, and Non-Unit Bus

We adopt constant impedance load models [41]. For $k \in \mathbb{N}_{\rm L}$, the model of the kth load is given by

$$\boldsymbol{i}_{[k]} = \boldsymbol{Y}_{[k]}\boldsymbol{v}_{[k]}, \quad k \in \mathbb{N}_{\rm L} \tag{4.7}$$

where $\boldsymbol{Y}_{[k]}$ denotes the admittance of the load associated with the kth bus.

Next, the model of the PV generators is given. First of all, we assume that all PV generators in every PV power plant are identical. Then the power generated by the PV power plant is the sum of the output of the all PV generators. Every PV generator is composed of a PV panel, a direct current (DC) /DC converter with a maximum power point tracking (MPPT) controller, and an inverter with a controller [42]. Due to the MPPT controller, the generated power from the converter is set to be constant. Since the dynamics of the inverter is significantly fast due to the existence of the controller [43], it is reasonable to assume that the output of the PV plant is given by constant power. Consequently, the model of the kth PV power plant is given by

$$\boldsymbol{i}^*_{[k]}\boldsymbol{v}_{[k]} = \boldsymbol{p}^{\rm const}_{[k]}, \quad k \in \mathbb{N}_{\rm P}$$

where $\boldsymbol{p}^{\rm const}_{[k]}$ denotes a constant of the power output.

Finally, from Kirchhoff's low, the model of the kth non-unit bus is given by

$$\boldsymbol{i}_{[k]} = \boldsymbol{0}, \quad k \in \mathbb{N}_{\rm N}. \tag{4.8}$$

4.2.3 System Model

Now, suppose that the power grid is managed by multiple independent system operators (ISOs) and each component is associated with a single ISO. Let $\mathbb{L}$ denote the index set of ISOs and $\mathcal{I}_l$ be the index of the components managed by the lth ISO. Then

$$\bigcup_{l \in \mathbb{L}} \mathcal{I}_l = \mathbb{N},$$

is satisfied, that is, there is no overlap among them.

Let $\Sigma_l^{(\mathrm{nl})}$ denote the nonlinear model of the components associated with the lth ISO. The model $\Sigma_l^{(\mathrm{nl})}$ can be written by

$$\Sigma_l^{(\mathrm{nl})}: \begin{cases} \dot{x}_l &= f_l(x_l, \boldsymbol{v}_l, \boldsymbol{i}_l, u_{\mathrm{s},l}, u_l) \\ 0 &= g(x_l, \boldsymbol{v}_l, \boldsymbol{i}_l) \\ y_l &= h_l(x_l, \boldsymbol{v}_l, \boldsymbol{i}_l) \end{cases} \tag{4.9}$$

where

$$x_l := \mathrm{col}(x_{[k]})_{k\in\mathcal{I}_l}, \quad \boldsymbol{v}_l := \mathrm{col}(\boldsymbol{v}_{[k]})_{k\in\mathcal{I}_l}, \quad \boldsymbol{i}_l := \mathrm{col}(\boldsymbol{i}_{[k]})_{k\in\mathcal{I}_l},$$
$$u_{\mathrm{s},l} := \mathrm{col}(u_{\mathrm{s},[k]})_{k\in\mathcal{I}_l}, \quad u_l := \mathrm{col}(u_{[k]})_{k\in\mathcal{I}_l}, \quad y_l := \mathrm{col}(y_{[k]})_{k\in\mathcal{I}_l},$$

and f_l and g_l follow the dynamics of the components associated with the lth ISO. From (4.2), $\boldsymbol{i}_l$ is given by

$$\boldsymbol{i}_l := \sum_{m\in\mathcal{N}_l} \boldsymbol{Y}_{lm}\boldsymbol{v}_m \tag{4.10}$$

where $\mathcal{N}_l$ denotes the neighborhood of the components associated with the lth ISO and $\boldsymbol{Y}_{lm}$ denotes the corresponding admittance matrix. From (4.10), (4.9) can be written by

$$\Sigma_l^{(\mathrm{nl})}: \begin{cases} \dot{x}_l &= f_l\left(x_l, \boldsymbol{v}_l, \sum_{m\in\mathcal{N}_l} \boldsymbol{Y}_{lm}\boldsymbol{v}_m, u_{\mathrm{s},l}, u_l\right) \\ 0 &= g(x_l, \boldsymbol{v}_l, \sum_{m\in\mathcal{N}_l} \boldsymbol{Y}_{lm}\boldsymbol{v}_m) \\ y_l &= h_l(x_l, \boldsymbol{v}_l, \sum_{m\in\mathcal{N}_l} \boldsymbol{Y}_{lm}\boldsymbol{v}_m). \end{cases} \tag{4.11}$$

We here focus on small signal stability and it is suffices to consider the linear model

$$\Sigma_l: \begin{cases} \dot{x}_l &= A_l x_l + L_l \sum_{m\in\mathcal{N}_l} \boldsymbol{Y}_{lm}\boldsymbol{v}_m + B_{\mathrm{s},l}u_{\mathrm{s},l} + B_l u_l \\ 0 &= \Gamma_l x_l + \Lambda_l \sum_{m\in\mathcal{N}_l} \boldsymbol{Y}_{lm}\boldsymbol{v}_m \\ y_l &= C_l x_l + D_l \sum_{m\in\mathcal{N}_l} \boldsymbol{Y}_{lm}\boldsymbol{v}_m, \end{cases} \tag{4.12}$$

which is obtained from the linearization around an equilibrium. We consider the linear model (4.12) hereinafter.

Our goal is to establish a distributed design method for PSSs that amend the transient stability. The existing controller design approach [21] applies a traditional controller design method such as optimal controller design for the associated subsystem by treating the other part as a static system. As stated in Section 4.1, the stability of the whole power grid is not guaranteed when applying the existing approach. We will see the case where the power grid loses the stability in Section 4.4 numerically. To cope with the problem, we aim at build a systematic method for distributed design of PSSs. The next section proposes such a distributed design method via retrofit control developed in the previous chapters.

4.3 PSS Design based on Retrofit Control

This section provides a mathematical formulation of the PSS design problem stated in Section 4.2. Subsequently, we briefly review retrofit control in time-domain based on state-space representation for developing a solution to the formulated problem. At last, a PSS design approach based on time-domain retrofit control is proposed.

4.3.1 Problem Formulation

Let $\mathcal{X}_l$ denote the set of initial value of x_l that can be possibly taken. Our aim is to design a controller that provides u_l so as to satisfy

$$\|x_{\mathbb{L}}\|_2 \leq \gamma \epsilon_l, \quad {}^{\forall} l \in \mathbb{L} \tag{4.13}$$

for any $x_l(0) \in \mathcal{X}_l$ and

$$x_l(0) = [0^{\mathsf{T}} \ \cdots \ x_l(0)^{\mathsf{T}} \ \cdots \ 0^{\mathsf{T}}]^{\mathsf{T}}$$

where

$$x_{\mathbb{L}} := \mathrm{col}(x_l)_{l \in \mathbb{L}}, \tag{4.14}$$

$\epsilon_l > 0$ denotes a desired performance, and $\gamma > 0$ is an independent constant of u_l.

The measurement signal for the lth controller is restricted to only the local measurement output y_l, the interconnection signal $\{\boldsymbol{y}_m\}_{m \in \mathcal{N}_l}$, and the supplementary control input $u_{\mathrm{s},l}$ alone. More specifically, the control input u_l is given by

$$u_l = \mathcal{K}_l(y_l, \{\boldsymbol{v}_m\}_{m \in \mathcal{N}_l}, u_{\mathrm{s},l}), \quad l \in \mathbb{L} \tag{4.15}$$

with a controller $\mathcal{K}_l$. Moreover, we assume that all controllers are designed in a distributed fashion. The controller $\mathcal{K}_l$ depends only on the elements of the set

$$\Theta_l := \{A_l, B_{\mathrm{s},l}, B_l, C_l, D_l, L_l, \mathit{\Gamma}_l, \mathit{\Lambda}_l, \{\boldsymbol{Y}_{lm}\}_{m \in \mathcal{N}_l}\}.$$

Based on the conditions, the problem is formulated as follows.

Problem: Consider the power gird consisting of Σ_l for $l \in \mathbb{L}$ of which dynamics is represented as (4.12). It is assumed that the power grid is stable when $u_l = 0$ for any $l \in \mathbb{L}$. Design $\mathcal{K}_l$ in (4.15) for $l \in \mathbb{L}$ so as to satisfy the following conditions:

1. The whole power grid becomes stable.
2. The performance criterion (4.13) holds.
3. Each control input can be represented by (4.15).
4. Each controller $\mathcal{K}_l$ is designed based only on their corresponding system parameters of Θ_l.

4.3.2 Hierarchical State-Space Expansion for Retrofit Control in Time-Domain

We consider applying the retrofit control approach to the problem formulated above. However, Assumption 1, which has been made throughout the previous chapters, does not necessarily hold in power systems. To resolve this issue, hierarchical state-space expansion for retrofit control in the time-domain is briefly reviewed in this subsection. It is shown that retrofit control in time-domain does not require Assumption 1 but provides us the same advantage as in the frequency-domain. We first show the important lemma for the following discussion.

Lemma 1 *For the systems*

$$\begin{cases} \dot{x} = Ax + B_0 u_0 + \hat{B} u \\ y = Cx \end{cases} \tag{4.16}$$

and

$$\begin{cases} \dot{\hat{\xi}} = \hat{A}\hat{\xi} + \hat{B}\hat{w} \\ \dot{\xi} = A\xi + (A - \hat{A})\hat{\xi} + B_0 w \\ y = Cx \end{cases} \tag{4.17}$$

where $\hat{A}$ is any compatible matrix. If

$$x(0) = \xi(0) + \hat{\xi}(0)$$

and

$$u_0 = w, \quad u = \hat{w}$$

then

$$x(t) = \xi(t) + \hat{\xi}(t), \quad {}^{\forall}t \geq 0 \tag{4.18}$$

is satisfied for any w and $\hat{w}$.

Proof: The sum of the dynamics in (4.17) leads to

$$\dot{\xi}(t) + \dot{\hat{\xi}}(t) = A\left(\xi(t) + \hat{\xi}(t)\right) + Bw + \hat{B}\hat{w}.$$

From the assumption, (4.18) is satisfied. □

Lemma 1 implies that the state x can be obtained by summing of the states ξ and $\hat{\xi}$. Due to Lemma 1, we can analyze the stability and $\mathcal{L}_2$ performance of x through the analysis on ξ and $\hat{\xi}$. We call the system representation (4.17) as hierarchical state-space expansion of the system (4.16).

It is assumed that a controller for $w = u_0$ is attached in advance and its dynamics is given by

$$\begin{cases} \dot{\xi}_{\mathrm{c}} = A_{\mathrm{c}}\xi_{\mathrm{c}} + B_{\mathrm{c}}y \\ \quad\;\; = A_{\mathrm{c}}\xi_{\mathrm{c}} + B_{\mathrm{c}}C(\xi + \hat{\xi}) \\ w = C_{\mathrm{c}}\xi_{\mathrm{c}} + D_{\mathrm{c}}y \\ \quad\;\; = C_{\mathrm{c}}\xi_{\mathrm{c}} + D_{\mathrm{c}}C(\xi + \hat{\xi}). \end{cases} \tag{4.19}$$

Then the dynamics of ξ and ξ_{c} is represented as

$$\begin{bmatrix} \dot{\xi} \\ \dot{\xi}_{\mathrm{c}} \end{bmatrix} = A_{\mathrm{CL}} \begin{bmatrix} \xi \\ \xi_{\mathrm{c}} \end{bmatrix} + R_0\hat{\xi}$$

where

$$A_{\mathrm{CL}} := \begin{bmatrix} A + BD_{\mathrm{c}}C & BC_{\mathrm{c}} \\ B_{\mathrm{c}}C & A_{\mathrm{c}} \end{bmatrix}, \quad R_0 := \begin{bmatrix} A - \hat{A} + BD_{\mathrm{c}}C \\ B_{\mathrm{c}}C \end{bmatrix}.$$

The following lemma gives a controller design criterion for guaranteeing the stability of the system (4.17).

Lemma 2 *Assume that A_{CL} is stable. Consider the controller*

$$\hat{K} : \begin{cases} \dot{\hat{\xi}}_{\mathrm{c}} = \hat{A}_{\mathrm{c}}\hat{\xi}_{\mathrm{c}} + \hat{B}_{\mathrm{c}}\hat{C}\hat{\xi} \\ \hat{w} = \hat{C}_{\mathrm{c}}\hat{\xi}_{\mathrm{c}} + \hat{D}_{\mathrm{c}}\hat{C}\hat{\xi} \end{cases} \tag{4.20}$$

where $\hat{C} := C$. *If the matrix*

$$\hat{A}_{\mathrm{CL}} := \begin{bmatrix} \hat{A} + \hat{B}\hat{D}_{\mathrm{c}}\hat{C} & \hat{B}\hat{C}_{\mathrm{c}} \\ \hat{B}_{\mathrm{c}}\hat{C} & \hat{A}_{\mathrm{c}} \end{bmatrix}$$

is a stable matrix, then the entire system (4.17) *with the controllers* (4.19) *and* (4.20) *becomes stable.*

Proof: The whole system is represented as

$$\begin{bmatrix} \dot{\hat{\xi}} \\ \dot{\hat{\xi}}_{\mathrm{c}} \\ \dot{\xi} \\ \dot{\xi}_{\mathrm{c}} \end{bmatrix} = \begin{bmatrix} \hat{A}_{\mathrm{CL}} & \begin{bmatrix} 0 & 0 \\ 0 & 0 \end{bmatrix} \\ \begin{bmatrix} R_0 & 0 & 0 \end{bmatrix} & A_{\mathrm{CL}} \end{bmatrix} \begin{bmatrix} \hat{\xi} \\ \hat{\xi}_{\mathrm{c}} \\ \xi \\ \xi_{\mathrm{c}} \end{bmatrix}.$$

Because of the block triangular property of the matrix,

$$\sigma\left(\begin{bmatrix} \hat{A}_{\mathrm{CL}} & \begin{bmatrix} 0 & 0 \\ 0 & 0 \end{bmatrix} \\ \begin{bmatrix} R_0 & 0 & 0 \end{bmatrix} & A_{\mathrm{CL}} \end{bmatrix}\right) = \sigma\left(\hat{A}_{\mathrm{CL}}\right) \cup \sigma\left(A_{\mathrm{CL}}\right).$$

The assumption leads to the stability of the entire system. □

Lemma 2 implies that the controller (4.20) stabilizes the system (4.17) with the controller (4.19) as long as the upstream dynamics of (4.17) with the controller (4.20) is stable. Thanks to the cascade structure, the stability is assured with the controllers for the upstream part with respect to $\hat{\xi}$. As a result, the original system becomes stable by employing the control input that stabilizes the upstream parts provided by $\hat{K}$ from Lemma 1. A strategy to generate the control input is included in the discussion in the next subsection.

Finally, the following lemma is shown in terms of performance of the entire system.

Lemma 3 *Assume that* $\hat{A}_{\mathrm{CL}}$ *is a stable matrix and the initial values hold*

$$\hat{\xi}(0) = x(0), \quad \xi(0) = 0.$$

Suppose the controller (4.20) *is implemented. Then the bound of $\mathcal{L}_2$-norm of x is given by*

$$\|x\|_2 \leq \gamma_0 \hat{\epsilon}$$

where

$$\gamma_0 := \| [I \ 0] (sI - A_{\mathrm{CL}})^{-1} R_0 + I\|_\infty, \quad \hat{\epsilon} := \left\| e^{\hat{A}_{\mathrm{CL}} t} \hat{\xi}(0) \right\|_2$$

Proof: Let $x(s), \xi(s)$ and $\hat{\xi}(s)$ denote the functions of $x(t), \xi(t)$, and $\hat{\xi}(t)$ in the Laplace domain. Lemma 1 leads to the inequality

$$\begin{aligned} \|x(t)\|_2 &= \|x(s)\|_2 \\ &= \|\xi(s) + \hat{\xi}(s)\|_2 \\ &= \| [I \ 0] (sI - A_{\mathrm{CL}})^{-1} R_0 \hat{\xi}(s) + \hat{\xi}(s)\|_2 \\ &\leq \gamma_0 \|\hat{\xi}(s)\|_2 \\ &= \gamma_0 \hat{\epsilon} \end{aligned}$$

and hence the conclusion holds. □

It should be noted that γ_0 is an independent constant of the controller and $\hat{\epsilon}$ is dependent only on $\hat{A}_{\mathrm{CL}}$. This result implies that the size of the state x is possibly suppressed in the sense of the upper bound by designing a controller that effectively works for the upstream part in (4.17). We utilize these results to develop retrofit control in time-domain. In the next subsection, we propose a PSS design method via retrofit control in time-domain that the results seen in this subsection produce.

4.3.3 Proposed PSS Design Method

First of all, let us try to determine $\hat{K}$ in (4.20). From (4.12), we have

$$\boldsymbol{v}_{\mathbb{L}} := \Pi_{\mathbb{L}} x_{\mathbb{L}} \tag{4.21}$$

where $x_{\mathbb{L}}$ is the states of the entire system given as (4.14), and

$$\begin{aligned} \boldsymbol{v}_{\mathbb{L}} &:= \mathrm{col}(\boldsymbol{v}_l)_{l \in \mathbb{L}}, \quad \Pi_{\mathbb{L}} := -(\Lambda \boldsymbol{Y}_{\mathbb{L}})^{-1} \Gamma_{\mathbb{L}}, \\ \Lambda_{\mathbb{L}} &:= \mathrm{diag}(\Lambda_l)_{l \in \mathbb{L}}, \quad \Gamma_{\mathbb{L}} := \mathrm{diag}(\Gamma_l)_{l \in \mathbb{L}}. \end{aligned}$$

Substituting (4.21) to (4.12), we have the model of the whole power grid

$$\Sigma_{\mathbb{L}} : \begin{cases} \dot{x}_{\mathbb{L}} &= A_{\mathbb{L}} x_{\mathbb{L}} + B_{\mathrm{s},\mathbb{L}} u_{\mathrm{s},\mathbb{L}} + B_{\mathbb{L}} u_{\mathbb{L}} \\ y_{\mathbb{L}} &= C_{\mathbb{L}} x_{\mathbb{L}} \\ \dot{x}_{\mathrm{s}} &= C_{\mathrm{s}} x_{\mathbb{L}} \\ u_{\mathrm{s},\mathbb{L}} &= \kappa_{\mathrm{s}} a x_{\mathrm{s}} \end{cases}$$

where

$$\begin{aligned} &u_{\mathbb{L}} := \mathrm{col}(u_l)_{l\in\mathbb{L}}, \quad y_{\mathbb{L}} := \mathrm{col}(y_l)_{l\in\mathbb{L}}, \quad A_{\mathbb{L}} := \mathrm{diag}(A_l)_{l\in\mathbb{L}} + L_{\mathbb{L}} \boldsymbol{Y}_{\mathbb{L}} \Pi_{\mathbb{L}}, \\ &B_{\mathbb{L}} := \mathrm{diag}(B_l)_{l\in\mathbb{L}}, \quad B_{\mathrm{s},\mathbb{L}} := \mathrm{diag}(B_{\mathrm{s},l})_{l\in\mathbb{L}}, \quad L_{\mathbb{L}} := \mathrm{diag}(L_l)_{l\in\mathbb{L}}, \\ &C_{\mathbb{L}} := \mathrm{diag}(C_l)_{l\in\mathbb{L}} + D_{\mathbb{L}} \boldsymbol{Y}_{\mathbb{L}} \Pi_{\mathbb{L}}, \quad D_{\mathbb{L}} := \mathrm{diag}(D_l)_{l\in\mathbb{L}}, \end{aligned} \tag{4.22}$$

x_{s} denotes the state of the supplementary controller, C_{s} denotes the matrix associated with the aggregated frequency deviation, $a := \mathrm{col}(a_{[k]})_{k\in\mathbb{N}_{\mathrm{G}}}$, and $u_{\mathrm{s},\mathbb{L}} := \mathrm{col}(u_{\mathrm{s},l})_{l\in\mathbb{L}}$.

Now, set

$$\hat{K}_l := \left[\begin{array}{c|c} A_{\mathrm{c},l} & B_{\mathrm{c},l} \\ \hline C_{\mathrm{c},l} & D_{\mathrm{c},l} \end{array}\right]$$

and choose matrices $A_{\mathrm{c},l} B_{\mathrm{c},l}, C_{\mathrm{c},l}, D_{\mathrm{c},l}$ for $l \in \mathbb{L}$ according to the following criterion

$$\left\| e^{\hat{A}_{\mathrm{CL},l} t} x_l(0) \right\|_2 \leq \epsilon_l, \quad {}^\forall x_l(0) \in \mathcal{X}_l \tag{4.23}$$

where

$$\hat{A}_{\mathrm{CL},l} := \begin{bmatrix} A_l + B_l D_{\mathrm{c},l} C_l & B_l C_{\mathrm{c},l} \\ B_{\mathrm{c},l} C_l & A_{\mathrm{c},l} \end{bmatrix}.$$

The controller design problem is a standard $\mathcal{H}_2$ suboptimal control problem that can be readily solved using some techniques, e.g., linear matrix inequalities, (for example, see [44]). The following theorem holds.

Theorem 8 *Consider the system* (4.12)*. Design* $\hat{K}_l$ *according to the performance criterion* (4.23)*. Set* $\hat{A}_{\mathbb{L}}, \hat{B}_{\mathbb{L}}, \hat{C}_{\mathbb{L}}$, *and* γ *by*

$$\hat{A}_{\mathbb{L}} := \mathrm{diag}(A_l)_{l\in\mathbb{L}}, \quad \hat{B}_{\mathbb{L}} := \mathrm{diag}(B_l)_{l\in\mathbb{L}}, \quad \hat{C}_{\mathbb{L}} := \mathrm{diag}(C_l)_{l\in\mathbb{L}},$$

and

$$\gamma := \left\| [I\ 0](sI - A_{\mathbb{L},\mathrm{CL}})^{-1} R + I \right\|_\infty$$

where

$$A_{\mathbb{L},\mathrm{CL}} := \begin{bmatrix} A_{\mathbb{L}} & B_{\mathrm{s},\mathbb{L}}\kappa_{\mathrm{s}} a \\ C_{\mathrm{s}} & 0 \end{bmatrix}, \quad R := \begin{bmatrix} A_{\mathbb{L}} - \hat{A}_{\mathbb{L}} \\ C_{\mathrm{s}} \end{bmatrix}.$$

Further, let the controller (4.20) *as*

$$A_{\mathrm{c}} := \mathrm{diag}(A_{\mathrm{c},l})_{l\in\mathbb{L}}, \quad B_{\mathrm{c}} := \mathrm{diag}(B_{\mathrm{c},l})_{l\in\mathbb{L}},$$
$$C_{\mathrm{c}} := \mathrm{diag}(C_{\mathrm{c},l})_{l\in\mathbb{L}}, \quad D_{\mathrm{c}} := \mathrm{diag}(D_{\mathrm{c},l})_{l\in\mathbb{L}}.$$

Then the $\mathcal{L}_2$-norm of the state can be bounded by (4.13)*.*

Proof: Because $\hat{\xi}(0) = x(0)$,

$$\left\| e^{\hat{A}_{\mathrm{cl}}t}\hat{\xi}(0) \right\|_2 = \sum_{l\in\mathbb{L}} \left\| e^{\hat{A}_{\mathrm{cl},l}t} x_l(0) \right\|_2.$$

Thus, for arbitrary $x_0(0) \in \mathcal{X}_l$,

$$\left\| e^{\hat{A}_{\mathrm{cl}}t}\hat{\xi}(0) \right\|_2 = \left\| e^{\hat{A}_{\mathrm{cl},l}t} x_l(0) \right\|_2$$

is satisfied when

$$x(0) = [0^{\mathsf{T}}\ x_l(0)^{\mathsf{T}}\ 0^{\mathsf{T}}]^{\mathsf{T}}.$$

Lemma 3 indicates that

$$\begin{aligned} \|x_{\mathbb{L}}\|_2 &\le \gamma \left\| e^{\hat{A}_{\mathrm{CL}}t}\hat{\xi}(0) \right\|_2 \\ &= \gamma \left\| e^{\hat{A}_{\mathrm{CL},l}t} x_l(0) \right\|_2. \end{aligned}$$

The assumption leads to that

$$\|x\|_2 \le \gamma\epsilon_l$$

for any $x_0(0) \in \mathcal{X}_l$. □

Theorem 8 provides a design strategy for $A_{\mathrm{c},l}B_{\mathrm{c},l}, C_{\mathrm{c},l}, D_{\mathrm{c},l}$ so as to give a performance bound according to (4.13). Pursuing the procedure developed above, we can set $\hat{K}_l$ under the constraint on distributed design.

Next, we discuss implementation of the designed controllers. Since the measurement signal of the controllers is $\hat{C}\hat{\xi}$ as represented by (4.20) and $\hat{\xi}$ becomes a virtual signal, the measurement signal cannot be obtained. To resolve the difficulty, under the variable transformation

$$\begin{bmatrix} x_{\mathbb{L}} \\ \hat{x}_{\mathbb{L}} \end{bmatrix} = \begin{bmatrix} I & I \\ 0 & I \end{bmatrix} \begin{bmatrix} \hat{\xi} \\ \xi \end{bmatrix} \tag{4.24}$$

we consider the system

$$\begin{cases} \dot{x}_{\mathbb{L}} &= A_{\mathbb{L}} x_{\mathbb{L}} + B_{\mathrm{s},\mathbb{L}} u_{\mathrm{s},\mathbb{L}} + B_{\mathbb{L}} u_{\mathbb{L}} \\ \dot{x}_{\mathrm{s}} &= C_{\mathrm{s}} x_{\mathbb{L}} \\ u_{\mathrm{s},\mathbb{L}} &= \kappa_{\mathrm{s}} a x_{\mathrm{s}} \\ \dot{\hat{x}}_{\mathbb{L}} &= \hat{A}_{\mathbb{L}} \hat{x}_{\mathbb{L}} + (A_{\mathbb{L}} - \hat{A}_{\mathbb{L}}) x_{\mathbb{L}} + B_{\mathrm{s},\mathbb{L}} u_{\mathrm{s},\mathbb{L}}. \end{cases} \tag{4.25}$$

The inverse of the coordinate transformation (4.24) leads to that

$$\hat{\xi} = x_{\mathbb{L}} - \hat{x}_{\mathbb{L}}.$$

Therefore if $\hat{x}_{\mathbb{L}}$ in (4.25) is available in a distributed fashion then we can obtain the control input in (4.20) employing $\hat{x}_{\mathbb{L}}$. We refer to the system providing $\hat{x}$ as an output rectifier and discuss a design method for decentralized output rectifier.

Note that

$$A_{\mathbb{L}} - \hat{A}_{\mathbb{L}} = L_{\mathbb{L}} \boldsymbol{Y}_{\mathbb{L}} \Pi_{\mathbb{L}}$$

and since $A_{\mathbb{L}} - \hat{A}_{\mathbb{L}}$ does not hold block diagonal structure and $(A_{\mathbb{L}} - \hat{A}_{\mathbb{L}})x_{\mathbb{L}}$ cannot be created using $x_{\mathbb{L}}$ in a distributed fashion, it is impossible to design and implement a decentralized output rectifier providing $\hat{x}_{\mathbb{L}}$ using $x_{\mathbb{L}}$. To overcome the problem, we employ not the signal $x_{\mathbb{L}}$ but the interconnection signal $\boldsymbol{v}_{\mathbb{L}}$. The relation

$$\begin{aligned} (A_{\mathbb{L}} - \hat{A}_{\mathbb{L}}) x_{\mathbb{L}} &= L_{\mathbb{L}} \boldsymbol{Y}_{\mathbb{L}} \Pi_{\mathbb{L}} x_{\mathbb{L}} \\ &= L_{\mathbb{L}} \boldsymbol{Y}_{\mathbb{L}} \boldsymbol{v}_{\mathbb{L}} \\ &= \mathrm{col} \left(L_l \textstyle\sum_{m \in \mathcal{N}_l} \boldsymbol{Y}_{lm} \boldsymbol{v}_m \right)_{l \in \mathbb{L}}, \end{aligned} \tag{4.26}$$

leads us to following theorem.

Theorem 9 *For the systems* (4.25) *and*

$$\begin{cases} \dot{x}_{\mathbb{L}} &= A_{\mathbb{L}} x_{\mathbb{L}} + B_{\mathrm{s},\mathbb{L}} u_{\mathrm{s},\mathbb{L}} + B_{\mathbb{L}} u_{\mathbb{L}} \\ \dot{x}_{\mathrm{s}} &= C_{\mathrm{s}} x_{\mathbb{L}} \\ u_{\mathrm{s},\mathbb{L}} &= \kappa_{\mathrm{s}} a x_{\mathrm{s}} \\ \dot{\hat{x}}_{\mathbb{L}} &= \hat{A}_{\mathbb{L}} \hat{x}_{\mathbb{L}} + L_l \textstyle\sum_{m \in \mathcal{N}_l} \boldsymbol{Y}_{lm} \boldsymbol{v}_m + B_{\mathrm{s},\mathbb{L}} u_{\mathrm{s},\mathbb{L}}, \quad l \in \mathbb{L}, \end{cases} \tag{4.27}$$

set the initial values

$$\hat{x}_{\mathbb{L}}(0) = 0$$

and

$$\hat{x}_l(0) = 0, \quad l \in \mathbb{L}.$$

Then

$$\hat{x}_{\mathbb{L}}(t) = \mathrm{col}(\hat{x}_l(t))_{l\in\mathbb{L}}, \quad {}^{\forall}t \geq 0$$

is satisfied for any control input $u_{\mathbb{L}}$*.*

Proof: Let $\hat{e}$ the error and its dynamics is given by

$$\hat{e} := \hat{x}_{\mathbb{L}} - \mathrm{col}(\hat{x}_l)_{l\in\mathbb{L}}.$$

From (4.21), (4.22), and (4.26), the dynamics is simplified as

$$\dot{\hat{e}} = \hat{A}_{\mathbb{L}}\hat{e}.$$

The assumption on the initial condition leads to that

$$\hat{e}(t) = 0, \quad {}^{\forall}t \geq 0.$$

Thus, $\hat{x}_{\mathbb{L}}(t) = \mathrm{col}(\hat{x}_l(t))_{l\in\mathbb{L}}$ for any $t \geq 0$. □

Theorem 9 indicates that the decentralized output rectifiers

$$G_{\mathrm{R},l} : \begin{cases} \dot{\hat{x}}_l &= A_l\hat{x}_l + L_l \sum_{m\in\mathcal{N}_l} \boldsymbol{Y}_{lm}\boldsymbol{v}_m + B_{\mathrm{s},l}u_{\mathrm{s},l} \\ \hat{y}_l &= y_l - \left(C_l\hat{x}_l + D\sum_{m\in\mathcal{N}_l} \boldsymbol{Y}_{lm}\boldsymbol{v}_m\right) \end{cases}, \quad l \in \mathbb{L} \tag{4.28}$$

can generate the measurement output

$$\begin{aligned} \hat{C}\hat{\xi} &= \hat{C}\left(x_{\mathbb{L}} - \mathrm{col}(\hat{x}_l)_{l\in\mathbb{L}}\right) \\ &= \hat{y}_{\mathbb{L}} \end{aligned}$$

where $\hat{y}_{\mathbb{L}} := \mathrm{col}(\hat{y}_l)_{l\in\mathbb{L}}$ and enable us to create the control input in (4.20).

Finally, under the initial conditions

$$x(0) = \hat{\xi}(0), \quad \xi(0) = 0, \quad \hat{x}_l(0) = 0, \quad l \in \mathbb{L},$$

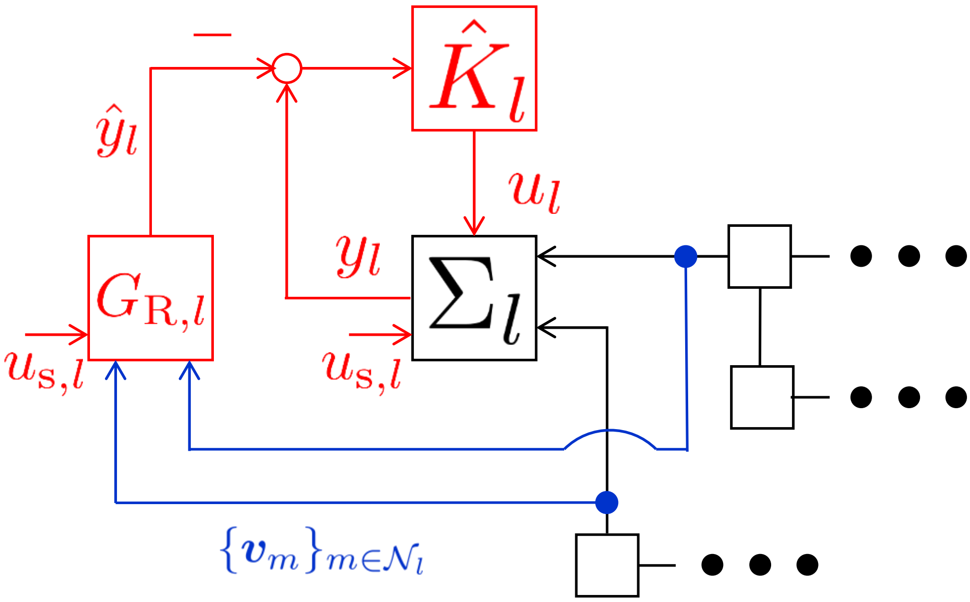

Fig. 4.2 Block diagram of the local system structure composed of $\Sigma_l, G_{\mathrm{R},l}$, and $\hat{K}_l$.

letting $A = A_{\mathbb{L}}, B = B_{\mathrm{s},\mathbb{L}}, \hat{B} = B_{\mathbb{L}}$, and $C = C_{\mathbb{L}}$ we can build an equivalent system consisting of $\Sigma_l, G_{\mathrm{R},l}, \hat{K}_l$ for $l \in \mathbb{L}$ to the whole system with (4.17) with (4.20), where Σ_l is given by (4.12), $G_{\mathrm{R},l}$ is given by (4.28), and

$$\hat{K}_l : \begin{cases} \dot{x}_{\mathrm{c},l} &= A_{\mathrm{c},l}x_{\mathrm{c},l} + B_{\mathrm{c},l}\hat{y}_l \\ u_{\mathrm{c},l} &= C_{\mathrm{c},l}x_{\mathrm{c},l} + D_{\mathrm{c},l}\hat{y}_l \end{cases}, \quad l \in \mathbb{L}. \tag{4.29}$$

It is shown that $\hat{K}_l$ can be designed only with the parameters A_l, B_l, C_l, and D_l from (4.23) and $G_{\mathrm{R},l}$ and $\hat{K}_l$ can be designed and implemented in a distributed fashion from (4.28) and (4.29). Fig. 4.2 depicts the block diagram corresponding to $\Sigma_l, G_{\mathrm{R},l}$, and $\hat{K}_l$.

We here summarize the obtained results and the proposed approach. The design method is given as follows. Choose $A_{\mathrm{c},l}B_{\mathrm{c},l}, C_{\mathrm{c},l}, D_{\mathrm{c},l}$ such that the performance criterion (4.23) is satisfied. Establish the controller $\mathcal{K}_l(y_l, \{\boldsymbol{v}_m\}_{m\in\mathcal{N}_l}, u_{\mathrm{s},l})$ as

$$\mathcal{K}_l : \begin{cases} G_{\mathrm{R},l} : \begin{cases} \dot{\hat{x}}_l &= A_l\hat{x}_l + L_l \sum_{m\in\mathcal{N}_l} \boldsymbol{Y}_{lm}\boldsymbol{v}_m + B_{\mathrm{s},l}u_{\mathrm{s},l} \\ \hat{y}_l &= y_l - \left(C_l\hat{x}_l + D_l \sum_{m\in\mathcal{N}_l} \boldsymbol{Y}_{lm}\boldsymbol{v}_m\right) \end{cases} \\ \hat{K}_l : \begin{cases} \dot{x}_{\mathrm{c},l} &= A_{\mathrm{c},l}x_{\mathrm{c},l} + B_{\mathrm{c},l}\hat{y}_l \\ u_{\mathrm{c},l} &= C_{\mathrm{c},l}x_{\mathrm{c},l} + D_{\mathrm{c},l}\hat{y}_l. \end{cases} \end{cases} \tag{4.30}$$

We can confirm that the conditions of the formulated problem are satisfied as follows.

1. Because the grid with the supplementary controller becomes stable, Lemma 2 implies that the entire system with the designed PSSs is stable.

2. Since the obtained whole system is equivalent to the system (4.12) with (4.20), Theorem 8 indicates that the performance criterion (4.13) is satisfied.

3. From the form of the design controller (4.30), it can be seen that the measurement signals are $y_l, \{\boldsymbol{v}_m\}_{m\in\mathcal{N}_l}$, and $u_{\mathrm{s},l}$.

4. From the design process of the controllers, only the local parameters in the set Θ_l are used and hence distributed design is achieved.

Finally, it should be remarked that the form of the retrofit controller (4.30) is exactly the same as that of retrofit controllers developed in the previous chapters when regarding Σ_l as the local system and $(\boldsymbol{v}_m, u_{\mathrm{s},l})$ as the interconnection signal from the environment. However, for the development of the controller (4.30), a retrofit controller in the time-domain, the assumption that the local system is stable is not made at all. Thus we can apply the retrofit control approach for power systems in which local systems are not necessarily stable.

4.4 Numerical Simulation

This section provides a numerical simulation showing the effectiveness of the proposed approach for control of power grids. PV-integrated EAST30 model is used and the gird is depicted in Fig. 4.3. The PV-integrated EAST30 model is composed of 137 buses, 30 generators, 31 loads, 30 PVs, and transmission facilities. The transmission line parameters of EAST30 model are given in [25]. Although no PV generators are installed into the original IEEJ EAST30 model, in order to simulate future power systems we place some PV power plants. The places of the buses where PV power plants are attached are determined according to the data of areas where large amount of PV is penetrated in the future Japanese power system [45]. Since the model of the generator has 13-dimensional states, the dimension of the whole grid reaches at 390. The PV generation is assumed to cover 6% of the total demand in the grid. The amount is supposed to be 30% of the FIT installed amount in Japan. The supplementary control is designed based on the following parameters

$$\kappa_{\mathrm{s}} = -1, \quad a_{[k]} = 1. \quad {}^{\forall}k \in \mathbb{N}_{\mathrm{G}}.$$

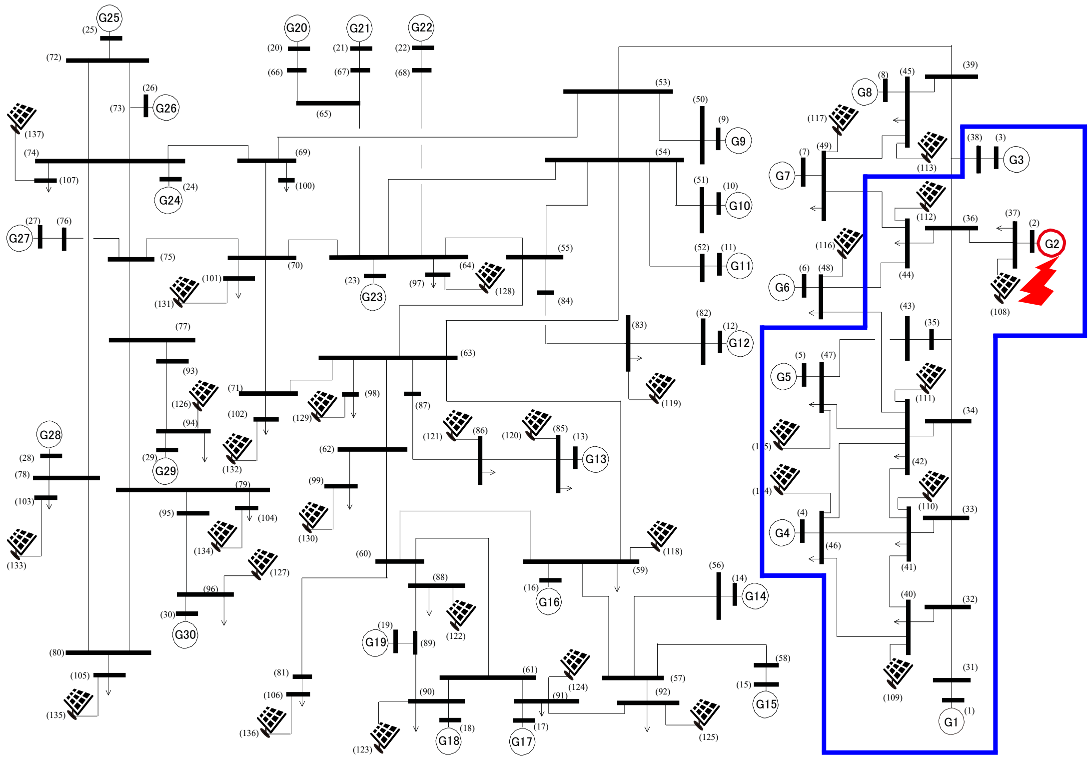

Fig. 4.3 PV-integrated IEEJ EAST 30-machine power system.

The whole grid is stable with the supplementary controller unless any additional controller is implemented.

The indices of the components are given by

$$
\begin{aligned}
&\mathbb{L} = \{1, 2\},\\
&\mathcal{I}_1 \cap \mathbb{N}_{\mathrm{G}} = \{1, \ldots, 5\},\\
&\mathcal{I}_1 \cap \mathbb{N}_{\mathrm{L}} = \{37, 40, 41, 42, 44\},\\
&\mathcal{I}_1 \cap \mathbb{N}_{\mathrm{P}} = \{112, 117, 122, 127, 132\},\\
&\mathcal{I}_1 \cap \mathbb{N}_{\mathrm{N}} = \{31, \ldots, 36, 38, 39, 43, 50, \ldots, 58, 60, \ldots, 68\},\\
&\mathcal{I}_2 = \{1, \ldots, N\} \setminus \mathcal{I}_1.
\end{aligned}
$$

Let us suppose a fault happening in the second generator. The model of the contingency is given by an initial disturbance injected into the angle of the corresponding generator, namely,

$$
x_{[k]}(0) = \begin{cases} 0.1e_1 & \text{if } k = 2, \\ 0 & \text{otherwise.} \end{cases}
$$

For the given power grid, consider attaching retrofit controllers developed in the previous sections. We design $\mathcal{K}_i$ in (4.30) for $\mathcal{I}_1$ utilizing the $\mathcal{H}_2$ optimal control where the objective function is given by

$$J_1 := \int_0^\infty \left(x_1^\mathsf{T} Q_1 x_1 + r u_1^\mathsf{T} u_1 \right) dt$$

where

$$Q_1 = q_{\delta,1} \hat{e}_1 \hat{e}_1^\mathsf{T} + q_{\omega,1} \hat{e}_2 \hat{e}_2^\mathsf{T} + q_1 I$$

and

$$\hat{e}_i := 1_{|\mathcal{I}_1 \cap \mathbb{N}_\mathrm{G}|} \otimes e_i,$$

1_M is the M-dimensional all-ones vector, $e_i \in \mathbb{R}^{13}$ for $i \in \{1,2\}$ is the canonical bases associated with the ith coordination, and $q_{\delta,1}, q_{\omega,1}, q_1$ and r are positive constants. It is notable that $q_{\delta,1}$ and $q_{\omega,1}$ are associated with the angle and the frequency, respectively. For the second region $\mathcal{I}_2$, we place no primary controller to the power grid. We have employed MATPOWER [46] on MATLAB R2017a for the following numerical simulations.

We consider the three cases: First, no controller is added except for the supplementary controller. Second, a PSS designed with the traditional approach, namely, single-machine infinite-bus system. Finally, a PSS designed with the proposed retrofit control approach. The free responses of all generators' frequency deviation for $t \in [0, 50]$ are shown in Fig. 4.4. It is shown that large oscillations happen when no control is added. The responses for $t \in [0, 1.5]$ under the traditional approach are shown in Fig. 4.5. We can see that the power grid losses its stability by attaching the controller. The responses under the proposed approach for $t \in [0.50]$ are shown in Fig. 4.6 where

$$q_1 = 1, \quad q_{\delta,1} = 10^3, \quad q_{\omega,1} = q_{\omega,0}, \quad r = 1.$$

with $q_{\omega,0} := 10^7$. The figure demonstrates that the system is kept to be stable even when attaching the primary controller. Furthermore, the responses for $t \in [0, 0.5]$ is shown in Fig. 4.7. The figure indicates that the peak of the frequency deviation is suppressed by the proposed approach from -0.0904 to -0.0753. In order to further reduce the peak of the frequency deviation, we next design a controller using the parameter

$$q_{\omega,1} = q_{\omega,0} \times 10^3.$$

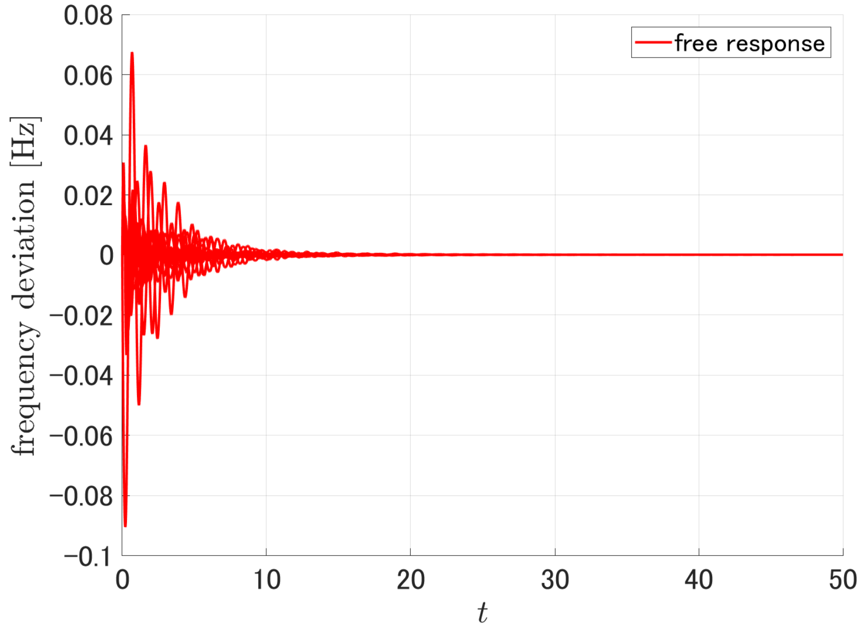

Fig. 4.4 Free responses of all generators' frequencies.

The responses with the newly designed controller are shown in Fig. 4.8. The figure indicates that the oscillation is still more reduced to -0.0505, which is 55% of the peak value without any controller. These results suggest that the proposed PSS design method is effective for improving damping performance of the power grid.

4.5 Chapter Summary

In this chapter, we have proposed a distributed design method for PSSs to cope with contingencies happening in power systems where a large amount of renewable energy resources is installed based on retrofit control. Since power grids into which large PV is introduced are susceptible to disturbance and readily destabilized, it is required to develop a novel method for designing PSSs that guarantee the stability of the whole power grid. While existing practical methods, including the single-machine infinite-bus based method, cannot theoretically guarantee the stability, retrofit control can give theoretical assurance of the stability. The proposed method is an extension of the existing retrofit control to be applicable for power systems. We have first provided a dynamical model of the power grid that consists of synchronous generators, loads, PV plants, and buses. It has been shown that the power system can be treated as a large-scale network system and the problem on distributed design of PSSs have been

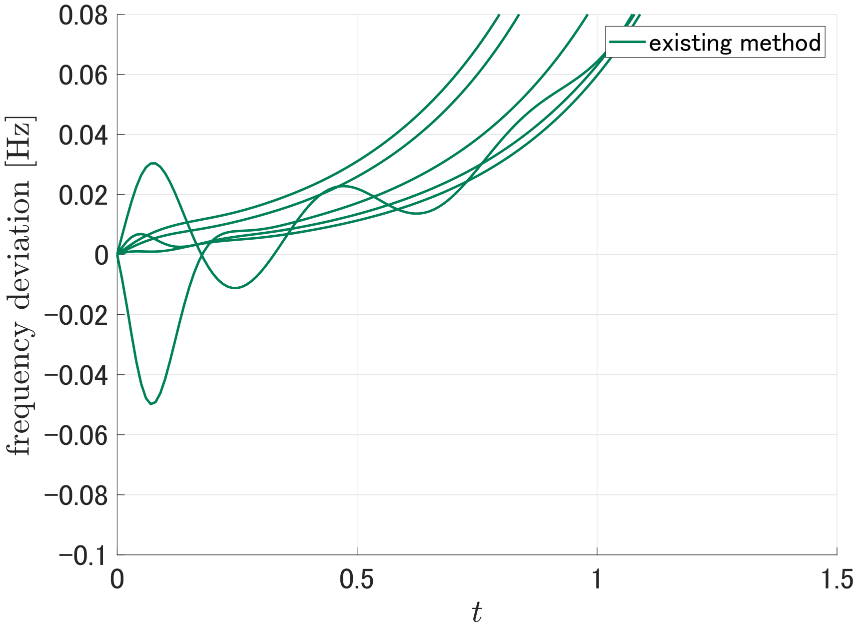

Fig. 4.5 Responses of all generators' frequencies with the controller designed based on the single-machine infinite-bus system.

mathematically formulated. We have derived a solution to the formulated problem based on retrofit control in the time-domain. Numerical simulations with PV-integrated EAST30 model have shown that the proposed approach not only stabilizes the power grid, which can be destabilized by a existing method using the single-machine infinite-bus model, but also sufficiently suppresses the frequency deviation.

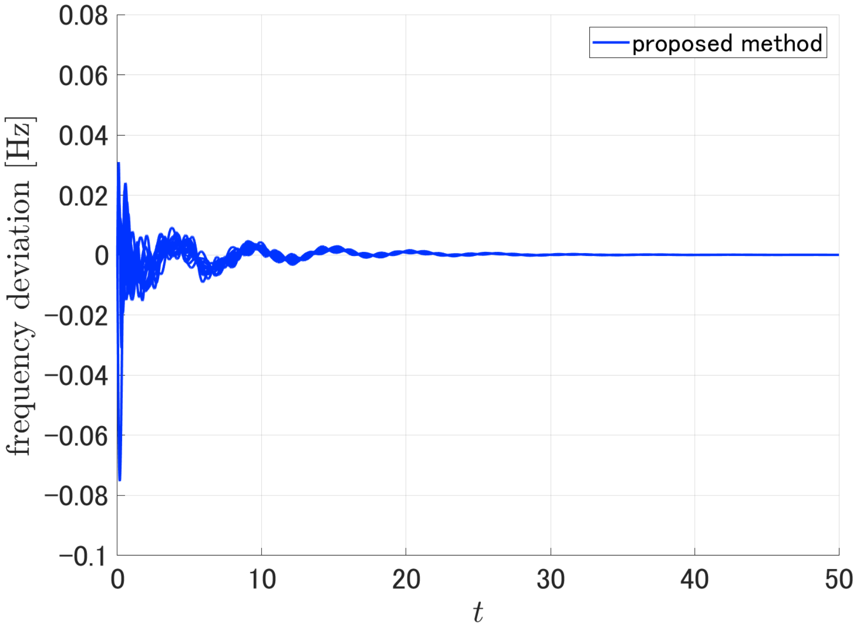

Fig. 4.6 Responses of all generators' frequencies of the closed-loop system with the proposed method when $q_{\omega,1} = q_{\omega,0}$.

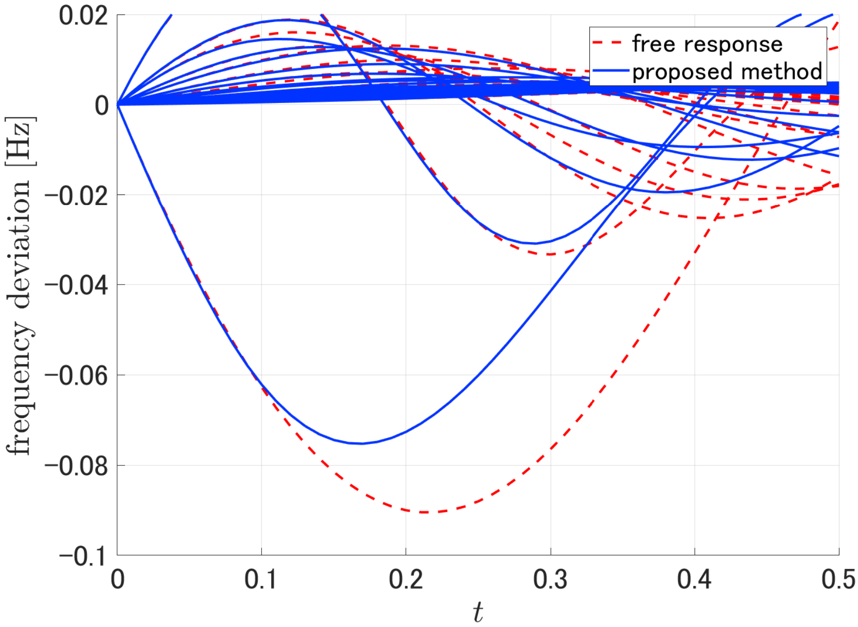

Fig. 4.7 Comparison of the responses without control and with the proposed method when $q_{\omega,1} = q_{\omega,0}$.

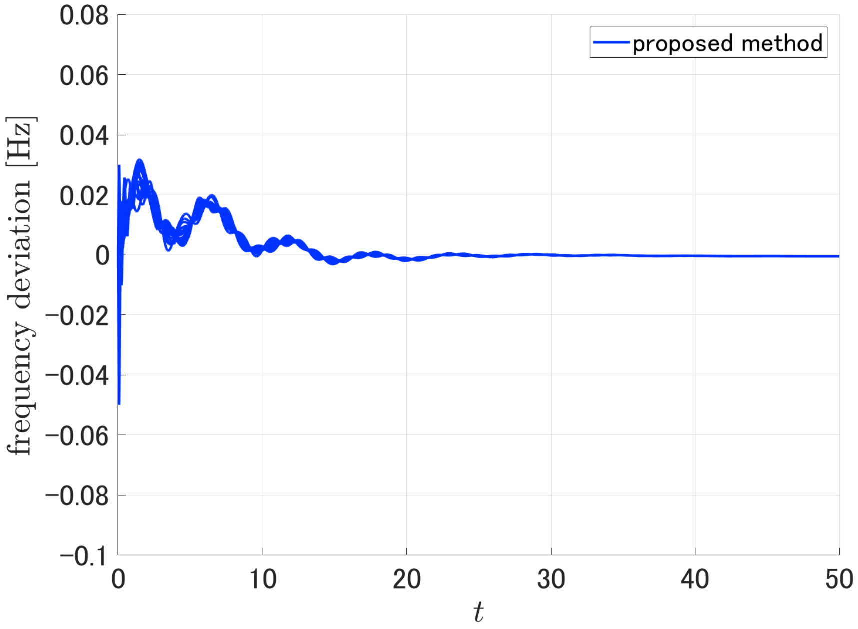

Fig. 4.8 Responses of all generators' frequencies of the closed-loop system with the proposed method when $q_{\omega,1} = q_{\omega,0} \times 10^3$.

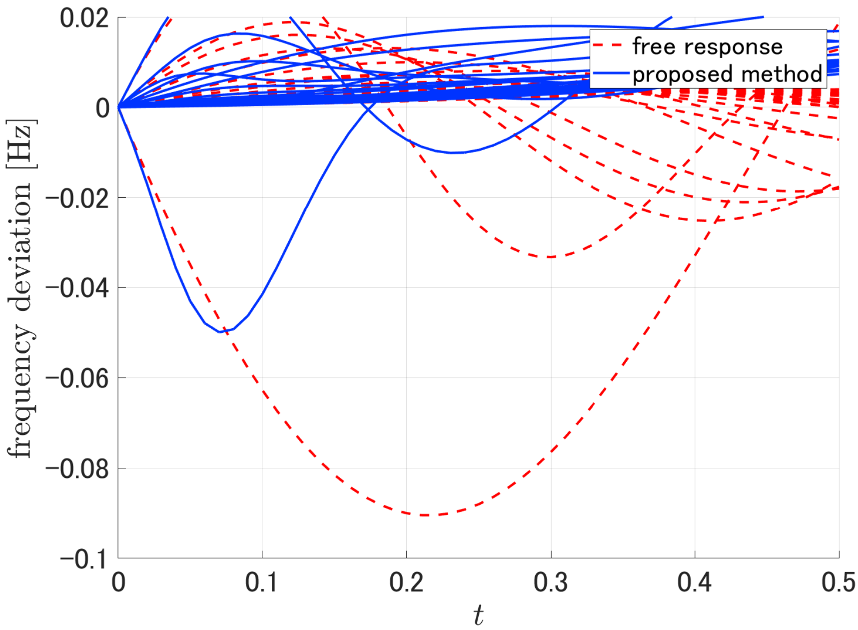

Fig. 4.9 Comparison of the responses without control and with the proposed method when $q_{\omega,1} = q_{\omega,0} \times 10^3$.

Chapter 5

Glocal Control of Network Systems via Hierarchical Representation

5.1 Introduction

We have developed a distributed design method for decentralized controllers. Based on the results seen in the previous chapters, we generalize the approach to glocal (global/local) control, where spatially distributed decentralized controllers and a central broadcasting controller cooperatively control the entire network system. We, in practice, take an objective-based approach to system modeling and control, e.g., subsystem identification for local decentralized control and modeling of aggregate system behavior for global broadcast control. We investigate such different kinds of control to realize desired system behavior.

The concept of glocal control has been already introduced in [26] but a systematic design of glocal controllers has not been established yet. We propose a novel glocal control method based on hierarchical representation where the original system is expressed as a hierarchical system. The approach for glocal control design is to consider an equivalent hierarchical system in which the upstream and downstream parts represent local and global behaviors, respectively. Then the original system is represented as a cascade system that consists of low dimensional systems. For the resulting system, we design local and global controllers for the upstream and downstream parts. The design procedure of controllers are independently performed and it indicates that the controller can be designed in a distributed manner.

Composite control, which is an existing approach employing multiple controllers for systems having multi time-scale, e.g., power plants [47–50], network systems composed of multiple robots [51], and transmission control protocol [52, 53]. The composite control requires the premise on which the whole system dynamics can be decomposed into two time-scales, slow and fast ones, by using the technique called singular perturbation [54, 55]. Under singular perturbation, each dynamics is treated as global and local dynamics that represent corresponding aggregated and local behaviors, respectively [56]. Nevertheless, it is not theoretically shown that the time-scale separation works well. The whole system, indeed, possibly loses the stability if the gap of the time-scales is insufficient, due to unanticipated interference among the controllers for the separated dynamics.

This chapter is organized as follows. We first see an example that motivates us to develop glocal control in Section 5.2. In Section 5.3, we give the system model treated in this chapter and the definition of hierarchical representation that is the key to developing glocal control. Further, we derive a characterization of hierarchical representation for a given system from the viewpoint of controllable subspace. In Section 5.4, we propose a distributed design method for designing glocal controllers based on hierarchical representation. Moreover, in Section 5.5, we see the effectiveness of the proposed glocal control through a numerical example of power system control. Finally, Section 5.6 concludes this chapter.

5.2 Motivating Example

First of all, a motivating example is shown to explain the framework of the proposed glocal control.

Let us consider a network composed of three second-order systems. Each subsystem is represented by

$$m_i\ddot{\theta}_i + d_i\dot{\theta}_i + v_i + u_i = 0, \quad i = 1, 2, 3$$

where v_i is the interconnected signal injected into the ith subsystem and u_i is the control input. The interconnection signal is represented by

$$v_i = \sum_{j \neq i} k_{ij}(\theta_i - \theta_j).$$

We assume that the system is homogeneous, that is, the coefficients are assumed to be the same as the other subsystems' ones and subscripts for all coefficients are omitted in the following. Then the entire system can be represented by

$$\dot{x} = \left(I \otimes \begin{bmatrix} 0 & 1 \\ 0 & -d/m \end{bmatrix} - L \otimes \begin{bmatrix} 0 & 0 \\ 1 & 0 \end{bmatrix} \right) x + I \otimes \begin{bmatrix} 0 \\ 1 \end{bmatrix} u$$

where

$$x := \sum_{i=1}^{3} e_i \otimes \begin{bmatrix} \theta_i \\ \dot{\theta}_i \end{bmatrix}, \quad u := \sum_{i=1}^{3} e_i u_i$$

with the canonical bases $e_i \in \mathbb{R}^3$ and

$$(L)_{ij} := \begin{cases} -k_{ij}/m, & i \neq j, \\ \sum_{j \neq i} k_{ij}/m, & i = j. \end{cases}$$

We suppose that the control input is represented as the sum of local control inputs and a global control input by

$$u = \sum_{i=1}^{3} e_i u_{\mathrm{L},i} + 1_3 u_{\mathrm{G}}$$

with all-ones vector $1_3 \in \mathbb{R}^3$.

We now consider the hierarchical system

$$\begin{cases} \dot{\xi}_i &= \begin{bmatrix} 0 & 1 \\ -3k/m & -d/m \end{bmatrix} \xi_i + \begin{bmatrix} 0 \\ 1 \end{bmatrix} u_{\mathrm{L},i}, \quad i = 1,2,3 \\ \dot{\xi}_0 &= \begin{bmatrix} 0 & 1 \\ 0 & -d/m \end{bmatrix} + \sum_{i=1}^{3} \begin{bmatrix} 0 & 0 \\ -k/m & 0 \end{bmatrix} \xi_i + \begin{bmatrix} 0 \\ 1 \end{bmatrix} u_{\mathrm{G}}. \end{cases}$$

Then it can be shown that

$$x(t) = (1_3 \otimes I)\xi_0(t) + \sum_{i=1}^{3} (e_i \otimes I)\xi_i(t), \quad {}^\forall t \geq 0$$

for all $u_{\mathrm{L},i}, u_{\mathrm{G}}$ provided that

$$x(0) = (1_3 \otimes I)\xi_0(0) + \sum_{i=1}^{3} (e_i \otimes I)\xi_i(0)$$

by simple algebra.

We consider designing local and global controllers

$$u_{\mathrm{L},i} = \mathcal{K}_{\mathrm{L}}(\xi_i), \quad i = 1,2,3$$

and

$$u_{\mathrm{G}} = \mathcal{K}_{\mathrm{G}}(\xi_0).$$

If the controllers stabilizes the corresponding system, the entire system is also stable due to the cascade structure. As a result, the original system is also stabilized. Then distributed design of glocal controllers is achieved.

Now a couple of questions are posed. The first question is what the condition is for existing such a hierarchical system of which the superposition of the states represents the original state exists. The second question is what the condition is for the hierarchical system to model after the original system. In the next section, we provide answers to the questions from the perspective of controllability.

5.3 Hierarchical Representation

In this section, we introduce the notion of hierarchical representation that is the key to developing distributed design of glocal controllers. First of all, we give a precise definition of hierarchical representation. Subsequently, we provide a characterization of hierarchical representation to establish a hierarchical representation for a given system.

5.3.1 Definition of Hierarchical Representation

We consider linear time-invariant systems represented by

$$\Sigma : \dot{x} = Ax + \sum_{i=1}^{N} B_i u_i + B_0 u_0 \tag{5.1}$$

where x is the state and u_i for $i = 1, \ldots, N$ are local control inputs and u_0 is global control input. Our aim here is to develop a distributed design method for local and global controllers for the control inputs.

Now we consider the following hierarchical system

$$\Xi : \begin{cases} \dot{\xi}_i &= \hat{A}_i \xi_i + \hat{B}_i u_i, \quad i = 1, \ldots, N \\ \dot{\xi}_0 &= \hat{A}_0 \xi_0 + \displaystyle\sum_{i=1}^{N} \hat{R}_i \xi_i + \hat{B}_0 u_0. \end{cases} \tag{5.2}$$

The definition of hierarchical representation is given as follows.

Definition 3 *The hierarchical system* (5.2) *is called a hierarchical representation of the original system* (5.1)*, when*

$$x(t) = P_0\xi_0(t) + \sum_{i=1}^{N} P_i\xi_i(t), \quad {}^{\forall}t \geq 0 \tag{5.3}$$

holds for any $u_0, u_1, \ldots, u_N$ *with full-column rank matrices* $P_0, P_1, \ldots, P_N$ *whose size are compatible with the dimension of the states under the initial condition*

$$x(0) = P_0\xi_0(0) + \sum_{i=1}^{N} P_i\xi_i(0).$$

According to the definition, the original state x can be represented as a superposition of the states ξ_i provided that the system (5.2) is a hierarchical representation of (5.1). Once a hierarchical representation is given, local controllers generating u_i for $i = 1, \ldots, N$ can be designed only with the parameters $\hat{A}_i$ and $\hat{B}_i$ and a global controller can be designed only with $\hat{A}_0, \hat{R}_i, \hat{B}_0$ as well. In this sense, hierarchical representation greatly helps us to achieve distributed design of glocal controllers.

5.3.2 Characterization of Hierarchical Representation

We give a characterization of hierarchical representation in this subsection.

First, we give a condition for existence of hierarchical representation. The following theorem holds.

Theorem 10 *There exists a hierarchical representation of the system* Σ *in* (5.1) *if and only if*

$$\begin{cases} \mathcal{R}(A, P_i) \subset \operatorname{im} P_i + \operatorname{im} P_0, \quad i = 1, \ldots, N \\ \mathcal{R}(A, P_0) \subset \operatorname{im} P_0, \\ \operatorname{im} B_i \subset \operatorname{im} P_i, \quad i = 0, \ldots, N \end{cases} \tag{5.4}$$

holds.

Proof: Sufficiency is shown in the proof of Theorem 11 by constructing a specific hierarchical representation. we here show necessity in this proof.

Assume that Ξ is a hierarchical representation of Σ. Let

$$x_0 \in \operatorname{im} P_0$$

and

$$x(0) = x_0, \quad \xi_0(0) = P_0^\dagger x_0, \quad \xi_i(0) = 0$$

for $i = 1, \ldots, N$. Because Ξ is a hierarchical representation,

$$x(t) = P_0 \xi_0(t), \quad {}^\forall t \geq 0$$

holds for $u_i = 0$ for $i = 0, \ldots, N$. Thus

$$x(t) = e^{At} x_0 \in \operatorname{im} P_0, \quad {}^\forall t \geq 0.$$

Since $\operatorname{im} P_0$ is a closed subspace,

$$\lim_{t \to 0} \frac{e^{At} x_0 - x_0}{t} = A x_0 \in \operatorname{im} P_0.$$

Because x_0 is an arbitrary element in $\operatorname{im} P_0$, $\operatorname{im} P_0$ is an invariant subspace of A. Hence $\mathcal{R}(A, P_0) \subset \operatorname{im} P_0$.

Similarly, it can be shown that $\mathcal{R}(A, P_i) \subset \operatorname{im} P_0 + \operatorname{im} P_i$ for $i = 1, \ldots, N$ by taking $x_0 \in \operatorname{im} P_i$.

Finally, we show that $\operatorname{im} B_i \subset \operatorname{im} P_i$ for $i = 0, \ldots, N$. Fix $i \in \{1, \ldots, N\}$ and set $x(0) = 0$, $\xi_i(0) = 0$ for $i = 0, \ldots, N$, and $u_j = 0$ for $j \neq i$. Then

$$\dot{x}(0) = B_i u_i(0) \in \operatorname{im} B_i$$

for any u_i. On the other hand,

$$\begin{aligned}
\dot{x}(0) &= P_0 \dot{\xi}_0(0) + \sum_{i=1}^{N} P_i \dot{\xi}_i(0) \\
&= P_0 \left(\hat{A}_0 \xi_0(0) + \sum_{i=1}^{N} \hat{R}_i \xi_i(0) + \hat{B}_0 u_0(0) \right) + \sum_{i=1}^{N} P_i \left(\hat{A}_i \xi_i(0) + \hat{B}_i u_i(0) \right) \\
&= P_i \hat{B}_i u_i(0) \in \operatorname{im} P_i.
\end{aligned}$$

Because there exists u_i for any $\dot{x}(0) \in \operatorname{im} B_i$, $\operatorname{im} B_i \subset \operatorname{im} P_i$, for $i = 0, \ldots, N$. □

A signal-flow diagram of the hierarchical system Ξ is shown in Fig. 5.1 where Ξ_i corresponds to the dynamics of ξ_i for $i = 0, \ldots, N$. As shown in the figure, ξ_i for $i = 1, \ldots, N$ does not affect ξ_j for $j \neq i$ at all and the necessity indicates that the original system must hold the structure.

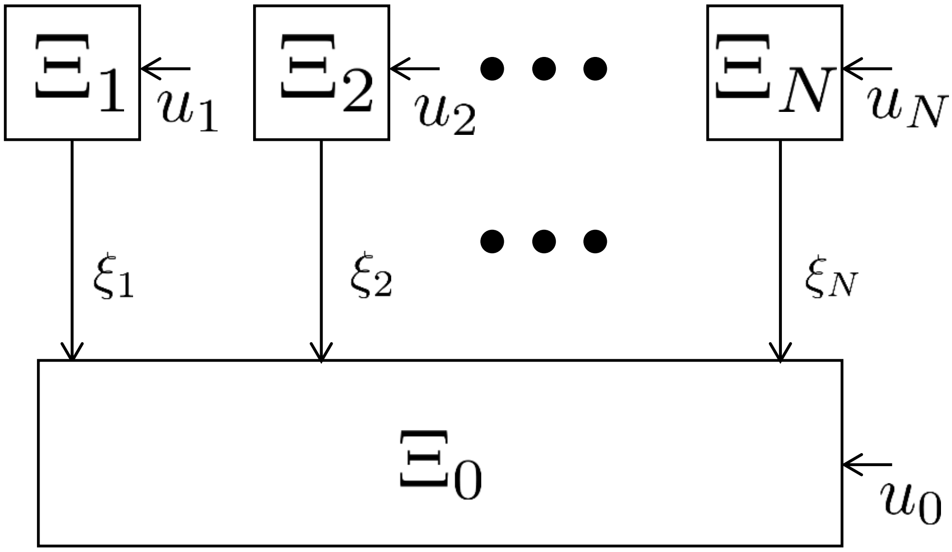

Fig. 5.1 Signal-flow diagram of Ξ.

We next give a characterization for Ξ to be a hierarchical representation of Σ. The following theorem holds.

Theorem 11 *The system Ξ is a hierarchical representation of Σ if and only if*

$$\begin{cases} \hat{A}_0 = P_0^{\dagger} A P_0 \\ AP_i - P_0\hat{R}_i - P_i\hat{A}_i = 0, \quad i = 1, \ldots, N \\ P_i\hat{B}_i = B_i, \quad i = 0, \ldots, N \end{cases} \tag{5.5}$$

holds.

Proof: (Sufficiency) First of all, we show that there exist matrices $\hat{A}_i$ and $\hat{R}_i$ for $i = 1, \ldots, N$ such that the condition (5.5) holds when the condition (5.4) is satisfied. Since

$$\mathcal{R}(A, P_i) \subset \operatorname{im} P_i + \operatorname{im} P_0, \quad i = 1, \ldots, N$$

holds,

$$\operatorname{im} AP_i \subset \operatorname{im} P_i + \operatorname{im} P_0, \quad i = 1, \ldots, N.$$

Hence there exist X_i, X_0 such that

$$AP_i = P_iX_i + P_0X_0.$$

Thus

$$\hat{A}_i = X_i, \quad \hat{R}_i = X_0$$

satisfy the condition (5.5).

Let us assume that the condition (5.5) holds. Define

$$e := x - P_0\xi_0 - \sum_{i=1}^{N} P_i\xi_i$$

and then

$$\begin{aligned}\dot{e} &= Ax - P_0\left(\hat{A}_0\xi_0 + \sum_{i=1}^{N}\hat{R}_i\xi_i\right) - \sum_{i=1}^{N} P_i\hat{A}_i\xi_i \\ &= Ax - P_0\hat{A}_0\xi_0 - \sum_{i=1}^{N}\left(P_0\hat{R}_i + P_i\hat{A}_i\right)\xi_i \\ &= Ax - P_0P_0^{\dagger}AP_0\xi_0 - \sum_{i=1}^{N} AP_i\xi_i.\end{aligned}$$

Since $\mathcal{R}(A, P_0) \subset \operatorname{im} P_0$,

$$P_0P_0^{\dagger}AP_0 = AP_0.$$

Therefore

$$\begin{aligned}\dot{e} &= Ax - AP_0\xi_0 - \sum_{i=1}^{N} AP_i\xi_i \\ &= A\left(x - P_0\xi_0 - \sum_{i=1}^{N} P_i\xi_i\right) \\ &= Ae.\end{aligned}$$

When $x(0) = P_0\xi_0(0) + \sum_{i=1}^{N} P_i\xi_i(0)$, $e(0) = 0$ and hence

$$e(t) = 0, \quad {}^{\forall}t \geq 0$$

for any u_i for $i = 0, \ldots, N$. Since there is no error, (5.3) holds. Thus Ξ is a hierarchical representation.

(Necessity) First we show that $\hat{A}_0 = P_0^{\dagger}AP_0, P_0\hat{B}_0 = B_0$. When $u_i = 0$ and $\xi_i = 0$ for $i = 1, \ldots, N$, $\xi_i(t) = 0$ for any $t \geq 0$. Thus then

$$x(t) = P_0\xi_0(t), \quad {}^{\forall}t \geq 0$$

for any u_0 provided that $x(0) = P_0\xi_0(0)$. Define

$$e_0 := P_0^\dagger x - \xi_0$$

and then

$$\begin{aligned}\dot{e}_0 &= P_0^\dagger Ax + P_0^\dagger B_0 u_0 - \hat{A}_0\xi_0 - \hat{B}_0 u_0 \\ &= P_0^\dagger AP_0P_0^\dagger x - \hat{A}_0\xi_0 + (P_0^\dagger B_0 - \hat{B}_0)u_0 \\ &= P_0^\dagger AP_0 e_0 + (P_0^\dagger AP_0 - \hat{A}_0)\xi_0 + (P_0^\dagger B_0 - \hat{B}_0)u_0.\end{aligned}$$

Since $e_0(t) = 0$ for ant $t \geq 0$, $\dot{e}_0(0) = 0$ for any $t \geq 0$. Because

$$\dot{e}_0(0) = (P_0^\dagger AP_0 - \hat{A}_0)\xi_0(0) + (P_0^\dagger B_0 - \hat{B}_0)u_0(0)$$

for any $\xi_0(0)$ and $u_0(0)$, $\hat{A}_0 = P_0^\dagger AP_0, P_0\hat{B}_0 = B_0$ holds. Similarly, it can be shown that $AP_i - P_0\hat{R}_i - P_i\hat{A}_i = 0$ and $P_i\hat{B}_i = B_i, \quad 1 = 0, \ldots, N$. □

Theorem 11 provides a characterization of hierarchical representations from the viewpoint of controllability. Some specific examples are given here.

Example 1: Let us suppose that

$$\operatorname{im} P_i \subset \operatorname{im} P_0, \quad i = 1, \ldots, N.$$

Then there exists $\hat{R}_i$ such that the condition in (5.5) is satisfied for any $\hat{A}_i$. Thus all hierarchical representations are parameterized by

$$\Xi : \begin{cases} \dot{\xi}_i = \hat{A}_i\xi_i + P_i^\dagger B_i u_i, \quad i = 1, \ldots, N \\ \dot{\xi}_0 = P_0^\dagger AP_0\xi_0 + P_0^\dagger \sum_{i=1}^{N} \left(AP_i - P_i\hat{A}_i\right)\xi_i + P_0^\dagger B_0 u_0 \end{cases}$$

with $\hat{A}_i$ for $i = 1, \ldots, N$. Note that this is exactly the same as the retrofit controller in the time-domain employed in Chapter 4 when $P_0 = I$.

Example 2: Let us suppose that

$$\operatorname{im} P_i \cap \operatorname{im} P_0 = \{0\}, \quad i = 1, \ldots, N.$$

Then $\hat{A}_i$ and $\hat{R}_i$ are uniquely determined. Accordingly,

$$\Xi : \begin{cases} \dot{\xi}_i &= X_i \xi_i + P_i^\dagger B_i u_i, \quad i = 1, \dots, N \\ \dot{\xi}_0 &= P_0^\dagger A P_0 \xi_0 + \sum_{i=1}^{N} X_{0i} \xi_i + P_0^\dagger B_0 u_0 \end{cases}$$

is the unique hierarchical representation where X_i and X_{0i} are the matrices

$$X_0 = (\overline{P}_0^\dagger P_i)^\dagger \overline{P}_0^\dagger A P_i, \quad X_{0i} = (\overline{P}_i^\dagger P_0)^\dagger \overline{P}_i^\dagger A P_i,$$

which satisfy

$$AP_i = P_0 X_{0i} + P_i X_i.$$

Through the following sections, we develop a glocal control method via hierarchical representation.

5.4 Glocal Control for Network Systems

In this section, we provide a distributed design procedure of glocal controllers via hierarchical representation.

5.4.1 Difficulty on Glocal Controllers Implementation

To clearly express the network structure, we consider a linear network system composed of N subsystems

$$G_i : \begin{cases} \dot{x}_i &= A_i x_i + L_i v_i + B_i u_i \\ w_i &= \Gamma_i x_i \\ y_i &= C_i x_i \end{cases}$$

with the network

$$w = Mv$$

where

$$w := \mathrm{col}(w_i), \quad v := \mathrm{col}(v_i).$$

We suppose that the control input can be decomposed by

$$\begin{aligned} u &:= \mathrm{col}(u_i) \\ &= \sum_{i=1}^{N} (e_i \otimes I) u_{\mathrm{L},i} + 1_N u_{\mathrm{G}} \end{aligned}$$

with local control inputs $u_{\mathrm{L},i}$ and a global control input u_{G}. Then the entire network system is written by

$$G_{\mathrm{all}} : \begin{cases} \dot{x} = Ax + Bu \\ y = Cx \end{cases} \tag{5.6}$$

where

$$A := \mathrm{diag}(A_i) + \mathrm{diag}(L_i) M \mathrm{diag}(\mathit{\Gamma}_i), \quad B := \mathrm{diag}(B_i), \quad C := \mathrm{diag}(C_i).$$

We now assume that Ξ in (5.2) is a hierarchical representation of G_{all} with matrices $P_0, P_1, \ldots, P_N$, where

$$P_i := e_i \otimes I.$$

It is easy to design controllers $\mathcal{K}_i$ for $i = 1, \ldots, N$ only with the model of G_i such that the system

$$\begin{cases} \dot{\xi}_i &= \hat{A}_i \xi_i + \hat{B}_i u_{\mathrm{L},i} \\ u_{\mathrm{L},i} &= \mathcal{K}_i(\hat{C}_i \xi_i) \end{cases} \tag{5.7}$$

is stable where $\hat{C}_i := C_i$. It is also easy to design a controller $\mathcal{K}_0$ such that the system

$$\begin{cases} \dot{\xi}_0 &= \hat{A}_0 \xi_0 + \hat{B}_0 u_{\mathrm{G}} \\ u_{\mathrm{G}} &= \mathcal{K}_0(\hat{C}_0 \xi_i) \end{cases} \tag{5.8}$$

is stable where

$$\hat{C}_0 := \sum_{i=1}^{N} (e_i^{\mathsf{T}} \otimes I) C_i.$$

Owing to the cascade structure of a hierarchical representation, stability of the entire system can be guaranteed if the control inputs in (5.7) and (5.8) can be implemented. The difficulty here is that the measurement signals $\hat{C}_i \xi_i$ cannot be directly measured. We will solve the problem in the next subsection.

5.4.2 Rectifier Design

The main idea to avoid the problem above is to design a linear function observer that produces the signals $\hat{C}_i\xi_i$, which we call a rectifier as an analogy of the rectifier in retrofit controller design.

The following theorem holds.

Theorem 12 *Consider the system* (5.6) *and assume that* Ξ *in* (5.2) *is a hierarchical representation of* $G_{\rm all}$. *Assume also that* $\mathcal{K}_i$ *for* $i = 0, \ldots, N$ *are designed so as to stabilize the systems* (5.7) *and* (5.8). *Then the system* $G_{\rm all}$ *with the controllers*

$$\begin{cases} u_{\mathrm{L},i} &= \mathcal{K}_i(\hat{C}_i\xi_i) \\ u_{\mathrm{G}} &= \mathcal{K}_0(y) \end{cases}$$

and

$$\mathcal{G}_i : \begin{cases} \dot{\phi}_i &= \mathscr{A}_i\phi_i + \mathscr{B}_{yi}y_i + \mathscr{B}_{vi}v_i + \mathscr{B}_{ui}u_i + \mathscr{B}_{u0}u_0 \\ \hat{\xi}_i &= \mathscr{C}_i\phi_i + \mathscr{D}_i y_i \end{cases}$$

for $i = 1, \ldots, N$ *is stable if* $\mathcal{G}_i$ *is a linear function observer of* Ξ *in* (5.2) *for* ξ_i.

Proof: We assume that $\mathcal{G}_i$ is a linear function observer for ξ_i. From the necessary and sufficient condition [57], it suggests that $\mathscr{A}_i$ is stable for any i and there exists a matrix U such that

$$\begin{aligned} &U \begin{bmatrix} \mathrm{diag}\left(\hat{A}_i\right) & 0 \\ \hat{R}_1 \cdots \hat{R}_N & \hat{A}_0 \end{bmatrix} - \mathrm{diag}\left(\mathscr{A}_i\right) U = \mathrm{diag}\left(\mathscr{B}_{yi}C_i + \mathscr{B}_{vi}\mathit{\Gamma}_i\right)[I \ \ P_0], \\ &[\mathrm{diag}\left(\mathscr{B}_{ui}\right) \ \ 1_N \otimes \mathscr{B}_0] = U \begin{bmatrix} \mathrm{diag}\left(\hat{B}_i\right) & 0 \\ 0 & \hat{B}_0 \end{bmatrix}, \\ &\mathrm{diag}\left(\mathscr{D}_i\right)[\mathrm{diag}(C_i) \ \ P_0] + \mathrm{diag}(\mathscr{C}_i)U = [I \ \ 0]. \end{aligned} \tag{5.9}$$

From the second equation in (5.9), it turns out that U has the form

$$U = [\mathrm{diag}\left(U_i\right) \ \ 1_N \otimes U_0]$$

as long as $\hat{B}_i$ is a column-full rank matrix for any i.

Define

$$e_i := U_i\xi_i + U_0\xi_0 - \phi_i.$$

Then because $\mathcal{G}_i$ is a linear function observer, the dynamics can be represented

$$\dot{e}_i = \mathscr{A}_i e_i$$

which is stable. Now since

$$\hat{\xi}_i = \xi_i - \mathscr{C}_i e_i$$

from the conditions in (5.9), the entire closed-loop system is composed of

$$\begin{cases} \dot{e}_i &= \mathscr{A}_i e_i \\ \dot{\xi}_i &= \hat{A}_i \xi_i + \hat{B}_i u_i \\ u_i &= \mathcal{K}_i(\hat{C}_i(\xi_i - \mathscr{C}_i e_i)) \end{cases}$$

for $i = 1, \ldots, N$, and

$$\begin{cases} \dot{\xi}_0 &= \hat{A}_0 \xi_0 + \sum_{i=1}^N \hat{R}_i \xi_i + \hat{B}_0 u_0 \\ u_{\mathrm{G}} &= \mathcal{K}_0 \left(\hat{C}_0 \left(\sum_{i=1}^N P_i \xi_i + P_0 \xi_0 \right) \right). \end{cases}$$

From the assumption and the hierarchical structure, the entire system is stable. □

Because the controllers can be designed based only on the local models, if we can design linear function observers only with the local model then distributed design of glocal controllers is achieved. In fact, the following theorem holds and states that there exist such rectifiers.

Theorem 13 *Assume that A_i and $\hat{A}_i$ are stable. Let*

$$\mathcal{G}_i : \begin{cases} \dot{\phi}_i &= \hat{A}_i \phi_i + (A_i - \hat{A}_i)\hat{x}_i + L_i v_i + P_i^\dagger P_0 \hat{B}_0 u_0 \\ \dot{\hat{x}}_i &= A_i \hat{x}_i + \hat{B}_i u_i + L_i v_i + P_i^\dagger P_0 \hat{B}_0 u_0 \\ \hat{\xi}_i &= -\hat{C}_i \phi_i + y_i. \end{cases}$$

Then $\mathcal{G}_i$ is a linear function observer for $C_i P_i \xi_i$.

Proof: It suffices to show that there exists a matrix U such that

$$U \begin{bmatrix} \mathrm{diag}\left(\hat{A}_i\right) & 0 \\ \hat{R}_1 \ \cdots \ \hat{R}_N & \hat{A}_0 \end{bmatrix} - \begin{bmatrix} \mathrm{diag}\left(\hat{A}_i\right) & \mathrm{diag}\left(A_i - \hat{A}_i\right) \\ 0 & \mathrm{diag}\left(A_i\right) \end{bmatrix} U$$
$$= \begin{bmatrix} 0 & \mathrm{diag}\left(L_i\right) \\ 0 & \mathrm{diag}\left(L_i\right) \end{bmatrix} \begin{bmatrix} \mathrm{diag}\left(\hat{C}_i\right) & \mathrm{diag}\left(\hat{C}_i\right) P_0 \\ M\mathrm{diag}\left(\Gamma_i\right) & M\mathrm{diag}\left(\Gamma_i\right) P_0, \end{bmatrix}$$

$$\begin{bmatrix} 0 & P_0\hat{B}_0 \\ \mathrm{diag}\left(\hat{B}_i\right) & P_0\hat{B}_0 \end{bmatrix} = U \begin{bmatrix} \mathrm{diag}\left(\hat{B}_i\right) & 0 \\ 0 & \hat{B}_0 \end{bmatrix},$$

and

$$[I\ 0] \begin{bmatrix} \mathrm{diag}\left(\hat{C}_i\right) & \mathrm{diag}\left(\hat{C}_i\right) P_0 \\ M\mathrm{diag}\left(\Gamma_i\right) & M\mathrm{diag}\left(\Gamma_i\right) P_0 \end{bmatrix} + \left[-\mathrm{diag}\left(\hat{C}_i\right)\right] U = \left[\mathrm{diag}\left(\hat{C}_i\right)\ 0\right].$$

Let us take

$$U = \begin{bmatrix} 0 & P_0 \\ I & P_0 \end{bmatrix}$$

and then simple algebra leads to the conclusion. □

All parameters in $\mathcal{G}_i$ are associated with G_i and hence it can be designed in a distributed manner.

The procedure of distributed design of glocal controllers via hierarchical representation is summarized as follows. First, we search for $P_0, \dots, P_N$ such that the conditions (5.4) hold for the system G_{all}. Next, parameters for a hierarchical representation are determined according to the conditions (5.4). For the given hierarchical representation, design controllers in (5.7) and (5.8). Finally, the resulting glocal controllers are implemented with the rectifiers.

5.5 Application to Power System Control

This section gives a numerical example to verify that the proposed control strategy efficiently works. The model used in the simulation is IEEJ EAST30 without PV plants shown in the previous chapter.

Let us suppose that a fault happens at the fifth generator. The fault is modeled by an initial deviation of the angle of the generator. To reduce the influence made by the contingency, we consider applying our method to the power system, where subsystems are determined according to the set of the generators within the area. The global controller $\mathcal{K}_{\mathrm{G}}$ generates the uniform actuation signal and sends it to all AVRs. On the other hand, the local controller $\mathcal{K}_{\mathrm{L},i}$ sends an actuation signal only to the corresponding AVRs.

Fig. 5.2 illustrated the trajectories of frequencies of the all generators in the grid. The response in the case where no control is applied is shown by the red lines. Large oscillation can be observed in this case of free response. The response in the case

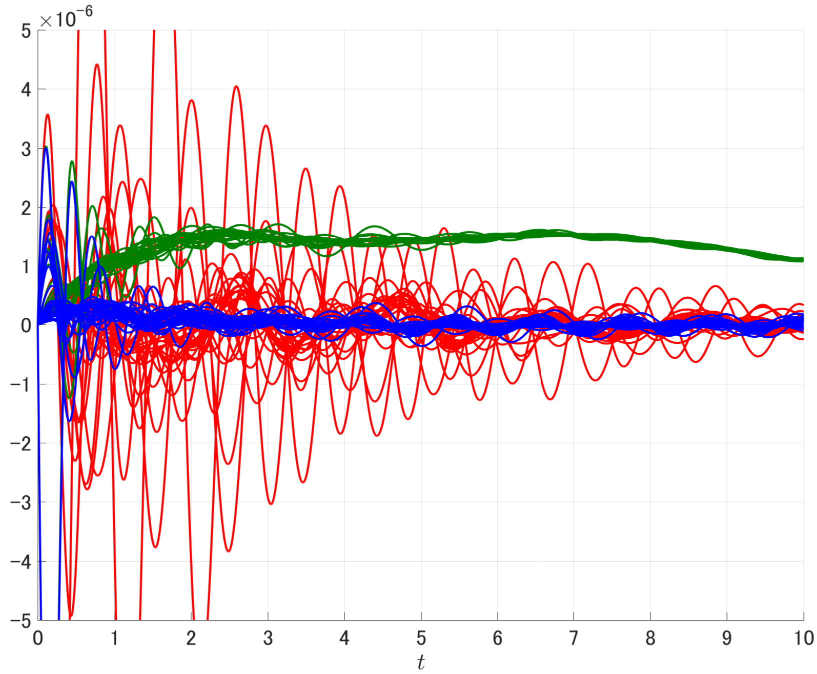

Fig. 5.2 Responses of all generators' frequencies, $t \in [0, 10]$. Red, green, and blue lines are obtained in the cases of no-control, retrofit control, proposed glocal control, respectively.

where retrofit control is applied is shown by the green lines. It can be observed that the trajectories after the 5 second similarly behave as compared to the trajectories of free responses. It is implied that incoherent dynamics can be suppressed by the retrofit controllers. Nevertheless, a uniform frequency deviation still remains and it slowly converges to the setpoint. The response in the case where the proposed glocal control is applied is shown by the blue lines. The glocal controllers are designed by heuristically ignoring the modeling error. The uniform frequency deviation, illustrated by the green lines, is greatly reduced by the newly introduced global controller, even though the stability is not assured in theory for the modeling error. It should be noted that the non-uniform dynamic is not stimulated by the global controller. These results indicates the efficiency of the proposed glocal control for control of real power systems.

5.6 Chapter Summary

In this chapter, we have proposed a distributed design method for global and local controllers for network systems. We have introduced a novel technique to represent the original system in a hierarchical one, called hierarchical representation. Thanks to the cascade structure of the hierarchical representation, it is enabled to distributedly design glocal controllers. We have shown that decentralized rectifiers can be also designed in a distributed manner. Finally, simulation results to show the effectiveness of the glocal control have been illustrated using the IEEJ EAST30 model.

Chapter 6

Conclusion

6.1 Summary of Results

This thesis has summarized the line of work on distributed design of controllers for dynamical network systems. Summaries in individual chapters are as follows:

First, in Chapter 2, a distributed design method of decentralized controllers based on the retrofit control approach has been proposed. We have considered a large-scale network system being stably operated where there are multiple operators with the aim of suppressing effects of disturbance injected into the network system by implementing subcontrollers. For the network system, the distributed design problem has been formulated by modeling the network system as an interconnected system composed of a local system and an environment. The definition of retrofit controllers has been given as the controllers that stabilize the interconnected system for any possible environment. It has been shown that all retrofit controllers can be parameterized based on Youla parameterization in the frequency domain. To investigate structure inside retrofit controllers, we have introduced two kinds of retrofit controllers, output-rectifying retrofit controllers and input-rectifying retrofit controllers. These controllers can be also parameterized by Youla parameter, and moreover, it can be reduced to be a parameter without any constraint. Thanks to the unconstrained parameterization, an optimal retrofit controller can be designed and consequently distributed design of decentralized controllers is achieved.

In Chapter 3, we have developed a retrofit controller design method without interconnection signal aiming at relaxing the assumption that the interconnection signal can be measured. We have considered the case where interconnection signal is unavailable and derive a parameterization of all state-feedback retrofit controllers without interconnection signal. It has been shown that a similar structure can be observed in state-feedback retrofit controllers to that of retrofit controllers with interconnection signal.

In Chapter 4, we have considered PSS design based on retrofit control for frequency control in power grids with renewable energy resources as an application of the proposed distributed design of decentralized controllers. We have given a mathematical model of EAST30 composed of synchronous machines, loads, PV power plants, non-unit buses, and tie-line networks. For synchronous machines, Park model is employed and each synchronous machine consists of a synchronous generator, an excitation system with AVR, and a turbine with governor. The loads and PV power plants are modeled as constant loads and constant power sources, respectively. We have shown that the power grid can be regarded as an interconnected system and formulated the problem of distributed design of PSSs. To treat unstable local systems, we have developed a retrofit controller design method in the time-domain. Numerical simulation has been shown to demonstrate the effectiveness of the proposed method.

As a generalization of the developed retrofit control, we have proposed a glocal control approach for distributedly designing local and global controllers based on hierarchical representation in Chapter 5. We have derived necessary and sufficient conditions for existing of hierarchical representation for a network system. Based on the hierarchical representation, we have proposed a glocal controller design method with rectifiers that preserve the hierarchical structure. Finally, the effectiveness of the proposed method has been verified through a numerical example.

6.2 Future Works

We have shown that all output-rectifying retrofit controllers with interconnection and all state-feedback output-rectifying retrofit controllers without interconnection signal have a structure inside the controller in Chapter 2 and 3. However, it is still unclear whether output-feedback output-rectifying retrofit controllers have a similar structure or not. One possible future direction is to generalize the result to the most general setting.

In addition, in Chapter 5, we have developed a glocal control approach for a given hierarchical representation. To search for a hierarchical representation for a given system is an interesting future work.

Bibliography

[1] S. H. Strogatz, "Exploring complex networks," *Nature*, vol. 410, pp. 268–276, 2001.

[2] P. Kundur, *Power System Stability and Control.* McGraw-Hill Education, 1994.

[3] M. D. Ilić and R. Jaddivada, "Multi-layered interactive energy space modeling for near-optimal electrification of terrestrial, shipboard and aircraft systems," *Annual Reviews in Control*, vol. 45, pp. 52–75, 2018.

[4] P. A. Ioannou and C. C. Chien, "Autonomous intelligent cruise control," *IEEE Transactions on Vehicular Technology*, vol. 42, no. 4, pp. 657–672, 1993.

[5] S. Wasserman and K. Faust, *Social Network Analysis.* Cambridge Univ. Press, 1994.

[6] A. V. Proskurnikov and R. Tempo, "A tutorial on modeling and analysis of dynamic social networks part I," *Annual Reviews in Control*, vol. 43, pp. 65–79, 2017.

[7] A. V. Proskurnikov and R. Tempo, "A tutorial on modeling and analysis of dynamic social networks part II," *Annual Reviews in Control*, vol. 45, pp. 166–190, 2018.

[8] G. Andersson *et al.*, "Causes of the 2003 major grid blackouts in north america and europe, and recommended means to improve system dynamic performance," *IEEE Transactions on Power Systems*, vol. 20, no. 4, pp. 1922–1928, 2005.

[9] D. D. Siljak, *Decentralized Control of Complex Systems.* Cambridge: Academic Press, 1991.

[10] N. Sandell, P. Varaiya, M. Athans, and M. Safonov, "Survey of decentralized control methods for large scale systems," *IEEE Transactions on Automatic Control*, vol. 23, no. 2, pp. 108–128, 1978.

[11] L. Bakule, "Decentralized control: An overview," *Annual Reviews in Control*, vol. 32, no. 1, pp. 87–98, 2008.

[12] C. Langbort and J. Delvenne, "Distributed design methods for linear quadratic control and their limitations," *IEEE Transactions on Automatic Control*, vol. 55, no. 9, pp. 2085–2093, 2010.

[13] E. V. Larsen and D. A. Swann, "Applying power system stabilizers part I: General concepts," *IEEE Transactions on Power Apparatus and Systems*, vol. PAS-100, no. 6, pp. 3017–3024, 1981.

[14] F. Farokhi, C. Langbort, and K. H. Johansson, "Optimal structured static state-feedback control design with limited model information for fully-actuated systems," *Automatica*, vol. 49, no. 2, pp. 326 – 337, 2013.

[15] Y.-S. Wang, N. Matni, and J. C. Doyle, "A system level approach to controller synthesis," 2017. [Online], Available: https://arxiv.org/abs/1610.04815v2.

[16] Y.-S. Wang, N. Matni, and J. C. Doyle, "Separable and localized system level synthesis for large-scale systems," *IEEE Transactions on Automatic Control*, 2019. (to appear).

[17] J. C. Doyle, N. Matni, N. Wang, J. Anderson, and S. Low, "System level synthesis: A tutorial," in *Proc. IEEE Conference on Decision and Control*, 2017.

[18] S. Baros and M. Ilić, "intelligent balancing authorities (iBAs) for transient stabilization of large power systems," in *Proc. IEEE PES General Meeting*, 2014.

[19] T. Ishizaki, T. Sadamoto, J. Imura, H. Sandberg, and K. H. Johansson, "Retrofit control: Localization of controller design and implementation," *Automatica*, vol. 95, pp. 336–346, 2018.

[20] T. Ishizaki, M. Koike, and J. Imura, "Transient response improvement for interconnected linear systems: Low-dimensional controller retrofit approach," *IEEE Transactions on Control of Network Systems*, pp. 1–1, 2018. (early access).

[21] H. F. Wang and F. J. Swift, "A unified model for the analysis of FACTS devices in damping power system oscillations. I. Single-machine infinite-bus power systems," *IEEE Transactions on Power Delivery*, vol. 12, no. 2, pp. 941–946, 1997.

[22] J. M. Carrasco, L. G. Franquelo, J. T. Bialasiewicz, E. Galvan, R. C. PortilloGuisado, M. A. M. Prats, J. I. Leon, and N. Moreno-Alfonso, "Power-electronic systems for the grid integration of renewable energy sources: A survey," *IEEE Transactions on Industrial Electronics*, vol. 53, no. 4, pp. 1002–1016, 2006.

[23] R. Takahashi and J. Tamura, "Frequency stabilization of small power system with wind farm by using flywheel energy storage system," in *IEEE International Symposium on Diagnostics for Electric Machines, Power Electronics and Drives*, pp. 393–398, 2007.

[24] P. Georgilakis, "Technical challenges associated with the integration of wind power into power systems," *Renewable and Sustainable Energy Reviews*, vol. 12, no. 3, pp. 852–863, 2008.

[25] The Institute of Electrical Engineers of Japan Power and Energy, 2016. [ONLINE]. Available:http://www.iee.jp/pes/?page_id=141.

[26] S. Hara, J. Imura, K. Tsumura, T. Ishizaki, and T. Sadamoto, "Glocal (global/local) control synthesis for hierarchical networked systems," in *Proc. IEEE Multi-Conference on Systems and Control*, pp. 107–112, 2015.

[27] K. Zhou, J. C. Doyle, and K. Glover, *Robust and Optimal Control.* Prentice Hall, 1996.

[28] D. Youla, H. Jabr, and J. Bongiorno, "Modern Wiener-Hopf design of optimal controllers–part II: The multivariable case," *IEEE Transactions on Automatic Control*, vol. 21, no. 3, pp. 319–338, 1976.

[29] D. S. Bernstein, *Matrix Mathematics: Theory, Facts, and Formulas*. Princeton University Press, 2 ed., 2009.

[30] F. Blaabjerg, Y. Yang, D. Yang, and X. Wang, "Distributed power-generation systems and protection," *Proceedings of the IEEE*, vol. 105, no. 7, pp. 1311–1331, 2017.

[31] Ministry of Economy, Trade, and Industry, "Feed-in Tariffs in Japan: Five years of achievements and future challenges," 2017. [Online]. Available: https://www.renewable-ei.org/en/activities/reports/img/pdf/20170810/REI_Report_20170908_FIT5years_Web_EN.pdf.

[32] Ministry of Economy, Trade, and Industry, "Long-term energy supply and demand outlook," 2015. [Online]. Available: http://www.meti.go.jp/english/press/2015/pdf/0716_01a.pdf.

[33] F. Blaabjerg, R. Teodorescu, M. Liserre, and A. V. Timbus, "Overview of control and grid synchronization for distributed power generation systems," *IEEE Transactions on Industrial Electronics*, vol. 53, no. 5, pp. 1398–1409, 2006.

[34] S. Eftekharnejad, V. Vittal, G. T. Heydt, B. Keel, and J. Loehr, "Impact of increased penetration of photovoltaic generation on power systems," *IEEE Transactions on Power Systems*, vol. 28, no. 2, pp. 893–901, 2013.

[35] B. Tamimi, C. Canizares, and K. Bhattacharya, "System stability impact of largescale and distributed solar photovoltaic generation: the case of Ontario Canada," *IEEE Transactions on Sustainable Energy*, vol. 4, no. 3, pp. 680–688, 2013.

[36] F. Blaabjerg, Z. Chen, and S. B. Kjaer, "Power electronics as efficient interface in dispersed power generation systems," *IEEE Transactions on Power Electronics*, vol. 19, no. 5, pp. 1184–1194, 2004.

[37] R. Ortega, M. Galaz, A. Astolfi, Y. Sun, and T. Shen, "Transient stabilization of multimachine power systems with nontrivial transfer conductances," *IEEE Transactions on Automatic Control*, vol. 50, no. 1, pp. 60–75, 2005.

[38] A. H. Etemadi, E. J. Davison, and R. Iravani, "A decentralized robust control strategy for multi-DER microgrids; Part I: Fundamental concepts," *IEEE Transactions on Power Delivery*, vol. 27, no. 4, pp. 1843–1853, 2012.

[39] F. Dörfler, M. R. Jovanović, M. Chertkov, and F. Bullo, "Sparsity-promoting optimal wide-area control of power networks," *IEEE Transactions on Power Systems*, vol. 29, no. 5, pp. 2281–2291, 2014.

[40] The Institute of Electrical Engineers of Japan, "Japanese power system model," *IEEJ Technical Report*, vol. 754, pp. 1–82, 1999. (in Japanese).

[41] K. Hatipoglu, I. Fidan, and G. Radman, “Investigating effect of voltage changes on static ZIP load model in a microgrid environment,” in *Proc. 2012 North American Power Symposium (NAPS)*, pp. 1–5, 2012.

[42] B. Subudhi and R. Pradhan, “A comparative study on maximum power point tracking techniques for photovoltaic power systems,” *IEEE Transactions on Sustainable Energy*, vol. 4, no. 1, pp. 89–98, 2013.

[43] H. Yuan, X. Yuan, and J. Hu, “Modeling of grid-connected VSCs for power system small-signal stability analysis in DC-link voltage control timescale,” *IEEE Transactions on Power Systems*, vol. 32, no. 5, pp. 3981–3991, 2017.

[44] T. Sato and K. Z. Liu, “LMI solution to general $\mathcal{H}_2$ suboptimal control problems,” *Systems & Control Letters*, vol. 36, no. 4, pp. 295–305, 1999.

[45] Ministry of Economy, Trade, and Industry, “Website for information disclosure on Feed-in Tariff in Japan,” 2017. [Online]. Available: http://www.enecho.meti.go.jp/category/saving_and_new/saiene/statistics/index.html (in Japanese).

[46] R. D. Zimmerman, C. E. Murillo-Sánchez, and R. J. Thomas, “MATPOWER: Steady-state operations, planning, and analysis tools for power systems research and education,” 2011.

[47] A. Chakrabortty and P. P. Khargonekar, “Introduction to wide-area control of power systems,” in *Proc. American Control Conference*, pp. 6758–6770, 2013.

[48] K. Seethalekshmi, S. N. Singh, and S. C. Srivastava, “Wide-area protection and control: Present status and key challenges,” in *Proc. National Power Systems Conference*, pp. 169–175, 2008.

[49] J. Xiao, F. Wen, C. Y. Chung, and K. P. Wong, “Wide-area protection and its applications - a bibliographical survey,” in *Proc. IEEE PES Power Systems Conference and Exposition*, pp. 1388–1397, 2006.

[50] A. M. Boker, T. R. Nudell, and A. Chakrabortty, “On aggregate control of clustered consensus networks,” in *Proc. American Control Conference*, pp. 5527–5532, 2015.

[51] R. Lozano, M. W. Spong, J. A. Guerrero, and N. Chopra, “Controllability and observability of leader-based multi-agent systems,” in *Proc. IEEE Conference on Decision and Control*, pp. 3713–3718, 2008.

[52] J. Kurose and K. Ross, *Computer Networking: A Top-Down Approach, 6th Ed.* Pearson Education Inc., 2012.

[53] K. Sakurama, E. I. Verriest, and M. Egerstedt, “Scalable stability and time-scale separation of networked, cascaded systems,” *IEEE Transactions on Control of Network Systems*, vol. 5, no. 1, pp. 321–332, 2018.

[54] P. Kokotović, H. K. Khalil, and J. O’Reilly, *Singular Perturbation Methods in Control: Analysis and Design.* Society for Industrial and Applied Mathematics, 1987.

[55] H. Khalil, “Output feedback control of linear two-time-scale systems,” *IEEE Transactions on Automatic Control*, vol. 32, no. 9, pp. 784–792, 1987.

[56] J. H. Chow and P. V. Kokotović, “Time scale modeling of sparse dynamic networks,” *IEEE Transactions on Automatic Control*, vol. 30, no. 8, pp. 714–722, 1985.

[57] T. Fortmann and D. Williamson, “Design of low-order observers for linear feedback control laws,” *IEEE Transactions on Automatic Control*, vol. 17, no. 3, pp. 301–308, 1972.

Acknowledgements

First and foremost, I fully thank my supervisor Jun-ichi Imura for his guidance and support and for providing me this precious study opportunity as a doctoral student in his laboratory. All of my research topics in this thesis began by his insightful suggestions, and carried out by his proper advice. I truly appreciate that he gave me the opportunity to pursue my own study and other projects.

I am deeply grateful to Assistant Professor Takayuki Ishizaki for his enthusiastic support, proper advice, and invaluable discussion that not only reveal the weakness in my study but make my research of great achievement. Without his support and widespread advice from mathematics to scientific writing and presentation, this work does not exist.

I am also very grateful to Associate Professor Tomohisa Hayakawa, Professor Kazuhiro Nakadai in Tokyo Institute of Technology, Assistant Professor Tomonori Sadamoto in the University of Electro-Communications, and Dr. Takahiro Kawaguchi in Tokyo Institute of Technology for valuable comments and suggestions.

I am indebted to my previous supervisors, Professor Emeritus Yutaka Yamamoto in Kyoto University and Professor Masaaki Nagahara in University of Kitakyushu who taught me the fundamentals of scientific research.

I am very grateful to Noriko Sugimoto and Akiho Setoguchi for their support of my life in the laboratory. Moreover, I thank current and past members of Imura, Hayakawa and Nakadai laboratories for many great discussions and all the good times. Finally, my thanks for my family will never be enough.

Hampei Sasahara
Tokyo Institute of Technology

List of Publications

Journal Papers

- Hampei Sasahara, Takayuki Ishizaki, Tomonori Sadamoto, Taisuke Masuta, Yuzuru Ueda, Hideharu Sugihara, Nobuyuki Yamaguchi, Jun-ichi Imura, "Damping performance improvement for PV-integrated power grids via retrofit control." *IFAC Control Engineering Practice,* 2019. (accepted for publication)

- Hampei Sasahara, Takayuki Ishizaki, Tomonori Sadamoto, Jun-ichi Imura, "Distributed design of local controllers for transient stabilization in power systems," *Transactions of the Society of Instrument and Control Engineers,* Vol. 53, No. 11, pp. 608–617, 2017. (in Japanese)

Refereed International Conference Papers

- Hampei Sasahara, Takayuki Ishizaki, Jun-ichi, Imura, "Parameterization of all state-feedback retrofit controllers," in *Proc. IEEE Conference on Decision and Control,* 2018.

- Hampei Sasahara, Takayuki Ishizaki, Masaki Inoue, Tomonori Sadamoto, Jun-ichi Imura, "A characterization of all retrofit controllers," in *Proc. American Control Conference,* 2018.

- Hampei Sasahara, Takayuki Ishizaki, Tomonori Sadamoto, Jun-ichi Imura, Henrik Sandberg, Karl Henrik Johansson, "Glocal control for network systems via hierarchical state-space expansion," in *Proc. IEEE Conference on Decision and Control,* 2017.